Electronic Supplementary Material (ESI) for ChemComm.

Electronic Supplementary Information

The primary dipole of flipper probes

José García-Calvo, Javier López-Andarias, Naomi Sakai and Stefan Matile*

Department of Organic Chemistry, University of Geneva, Geneva, Switzerland

Stefan.Matile@unige.ch

Table of Contents

1.	Materials and methods	S3
2.	Flipper synthesis	S5
	2.1. Synthesis of flippers **1** and **1'**	S5
	2.2. Synthesis of flippers **2** and **2'**	S6
	2.3. Synthesis of flippers **3** and **3'**	S10
3.	Solvatochromism	S14
4.	Fluorescence quantum yields	S19
5.	Dynamic-covalent ketone chemistry	S21
6.	Fluorescence spectroscopy in LUVs	S25
7.	Cellular studies	S30
8.	NMR spectra	S34
9.	Supplementary references	S47

1. Materials and methods

As in ref. S1. Briefly, reagents for synthesis were purchased from Fluka, Sigma-Aldrich, TCI and Across. Salts of the best grade available from Fluka or Sigma-Aldrich were used as received. Egg sphingomyelin (SM), 1,2-dioleoyl-*sn*-glycero-3-phosphocholine (DOPC) and Mini-extruder were purchased from Avanti Polar Lipids, cholesterol (CL) was purchased from Sigma-Aldrich. Column chromatography was carried out on silica gel 60 (SilicaFlash P60, 40-63 μm). Analytical (TLC) and preparative thin layer chromatography (PTLC) were performed on silica gel 60 (Merck, 0.2 mm) and silica gel GF (SiliCycle, 1 or 0.25 mm), respectively. Fluorescence measurements were performed using a FluoroMax-4 spectrofluorometer (Horiba Scientific) equipped with a stirrer and a temperature controller. All fluorescence spectra were background subtracted and corrected using correction factors supplied by the manufacturer. Melting points (Mp) were measured on a Melting Point M-565 (BUCHI). IR spectra were recorded on a Perkin Elmer Spectrum 100 FT-IR spectrometer (ATR, Golden Gate) and are reported as wavenumbers υ in cm^{-1} with band intensities indicated as s (strong), m (medium), w (weak), br (broad). All ^{1}H and ^{13}C NMR spectra were recorded (as indicated) on a Bruker 300 MHz, 400 MHz or 500 MHz spectrometer at room temperature (25 °C) and are reported as chemical shifts (δ) in ppm relative to TMS (δ = 0). Spin multiplicities are reported as a singlet (s), doublet (d), triplet (t) and quartet (q) with coupling constants (*J*) given in Hz, or multiplet (m). Broad peaks are marked as br. ^{1}H and ^{13}C resonances were assigned with the aid of additional information from 1D and 2D NMR spectra (H,H-NOESY, H,H-COSY, DEPT 135, HSQC and HMBC). ESI-MS for the characterization of new compounds was performed on an ESI API 150EX, APCI-MS was measured on Biotage Isolera™ Dalton 2000 system with APCI detector. ESI-HRMS was measured on Xevo G2-S Tof (Waters). All mass data are reported as mass-per-charge ratio *m/z* (intensity in %, [assignment]). The confocal laser scanning microscopy images of the cells were taken with a Leica SP5 STED. Fluorescence lifetime imaging microscopy (FLIM) was performed on a Nikon Eclipse Ti

A1R microscope upgraded with a FLIM kit from PicoQuant, equipped with a laser 485, PicoQuant, LDH-D-C-485 at 20 MHz and collecting the fluorescence between 550 and 650 nm.

Abbreviations. CL: Cholesterol; DMAP: 4-Dimethylaminopyridine; DOPC: Dioleyl-*sn*-glycero-3-phosphocholine; FLIM: Fluorescence lifetime imaging; LUVs: Large unilamellar vesicles; mCPBA: *meta*-Chloroperoxybenzoic acid; SM: Egg sphingomyelin; TBTA: Tris((1-benzyl-1*H*-1,2,3-triazol-4-yl)methyl)amine; TMSA: Trimethylsilylacetylene.

2. Flipper synthesis

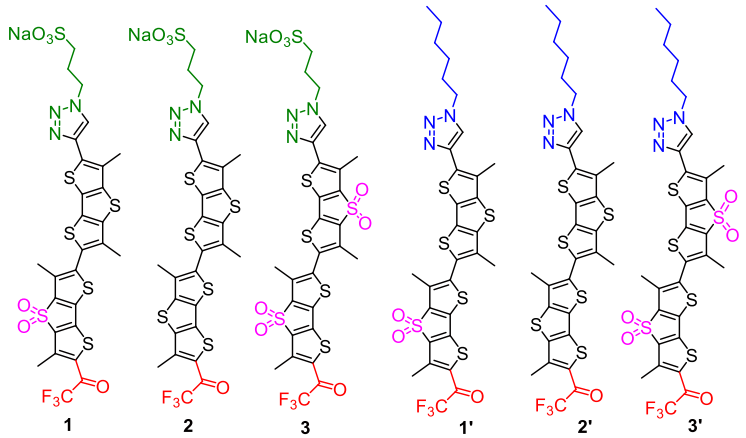

Fig. S1 Structures of the final compounds used in this study.

2.1. Synthesis of Flippers 1 and 1'

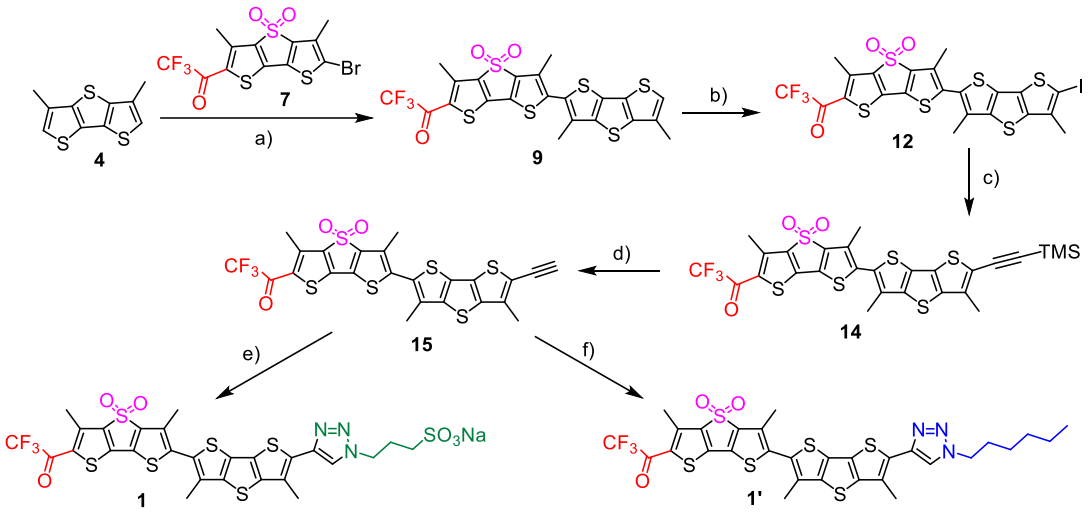

Scheme S1.[S1] (a) 1. *n*BuLi, THF, -78 ºC, 15 min; 2. Bu_3SnCl, -78 ºC to rt, 30 min; 3. **7**, $Pd(PPh_3)_4$, toluene/DMF, 80 ºC, 16 h, 4 - 23%; (b) NIS, AcOH, $CHCl_3$, rt, 0 °C for 30 min, rt for 1h; (c) TMSA, PPh_3, $PdCl_2(PPh_3)_2$, CuI, Et_3N, THF, 65 ºC, 12 h, 57%; (d) K_2CO_3, CH_2Cl_2/MeOH, rt, 2 h; (e) sodium 3-azidopropane-1-sulfonate, $CuSO_4 \cdot 5H_2O$, sodium ascorbate, TBTA, CH_2Cl_2/H_2O, rt, 12 h, 29%; (f) 1-azido hexane,[S1] $CuSO_4 \cdot 5H_2O$, sodium ascorbate, TBTA, CH_2Cl_2/H_2O, rt, 12 h, 86%.

Compounds 1 and 1' were prepared following the reported procedure.[S1]

2.2. Synthesis of flippers 2 and 2'

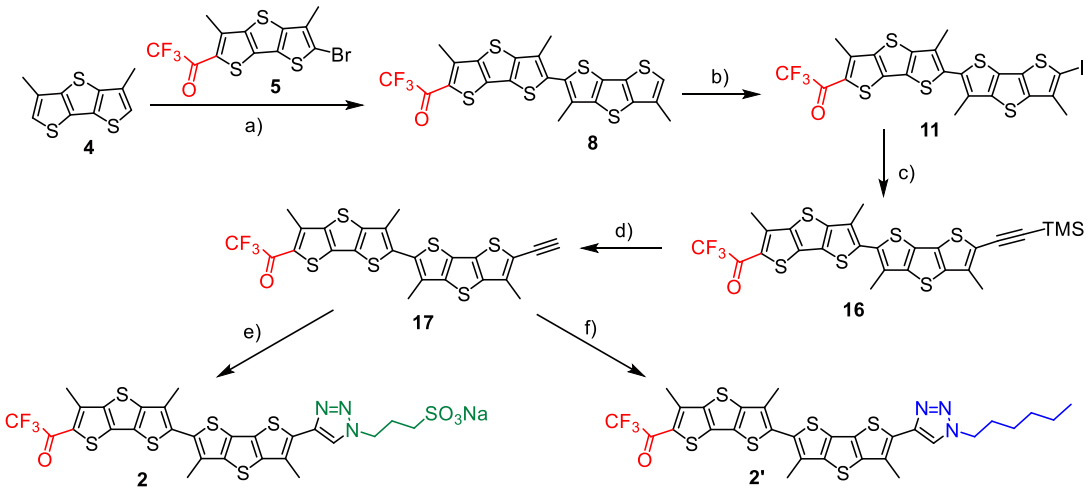

Scheme S2. (a) 1. *n*BuLi, THF, -78 ºC, 15 min; 2. Bu_3SnCl, -78 ºC to rt, 30 min; 3. **5**, $Pd(PPh_3)_4$, toluene/DMF, 80 ºC, 48 h, 25%; (b) NIS, AcOH, $CHCl_3$, rt, 0°C for 30 min, rt for 30 min; (c) TMSA, PPh_3, $PdCl_2(PPh_3)_2$, CuI, Et_3N, THF, 65 ºC, 12 h, 53%; (d) K_2CO_3, CH_2Cl_2/MeOH, rt, 2 h; (e) sodium 3-azidopropane-1-sulfonate, $CuSO_4 \cdot 5H_2O$, sodium ascorbate, TBTA, CH_2Cl_2/H_2O, rt, 2 h, 55%; (f) 1-azido hexane, $CuSO_4 \cdot 5H_2O$, sodium ascorbate, TBTA, CH_2Cl_2/H_2O, rt, 2 h, 53%.

Compound 4 was prepared following the reported procedure.[S2]

Compound 5 was prepared following the reported procedure.[S1]

Compound 8. To a solution of **4** (54 mg, 0.24 mmol) in dry THF (1.9 mL) under N_2 atmosphere, *n*BuLi (0.18 mL, 0.29 mmol, 1.6 M in hexane) was added dropwise at -78 °C, turning the solution green. To the mixture, Bu_3SnCl (65 µL, 0.24 mmol) was subsequently added and the reaction was immediately allowed to warm to rt, while turning colourless. After 30 min at rt, the solvents were evaporated *in vacuo* and the solids suspended in a mixture of dry toluene/DMF (1.2:0.2

mL). To this suspension, **5** (64 mg, 0.16 mmol) and $Pd(PPh_3)_4$ (9 mg, 0.008 mmol) were added. The mixture was stirred at 80 °C for 48 h, concentrated *in vacuo* and purified by column chromatography (SiO_2, CH_2Cl_2/pentane 1:3, R_f = 0.78) to give **8** (65 mg, 25%) as an orange solid. Mp: > 200 ºC; IR (neat): 2920 (m), 2895 (m), 1651 (s), 1431 (m), 1379 (m), 1188 (s), 1135 (s), 1029 (m), 854 (m), 752 (w), 727 (m); ^{1}H NMR (400 MHz, $CDCl_3$): 7.03 (s, 1H), 2.81 (s, 3H), 2.42 (s, 3H), 2.40 (s, 3H), 2.39 (s, 3H); ^{13}C NMR (126 MHz, $CDCl_3$): 174.2 (q, $^2J_{C\text{-}F}$ = 36.2 Hz, C=O), 148.2 (C), 145.5 (C), 144.1 (C), 143.1 (C), 142.5 (C), 137.9 (C), 135.4 (C), 131.1 (C), 130.7 (C), 129.1 (C), 128.3 (C), 126.2 (C), 122.1 (CH), 121.7 (C), 116.7 (q, $^1J_{C\text{-}F}$ = 290.8 Hz, CF_3), 16.9 (CH_3), 14.8 (CH_3), 14.2 (CH_3), 14.2 (CH_3); ^{19}F NMR (282 MHz, $CDCl_3$): -72.4; MS (APCI+): 543 (100, $[M+H]^+$).

Compound 11. To a solution of **8** (40 mg, 74 µmol) in chloroform (4 mL) at 0 °C, NIS (50 mg, 220 µmol) and AcOH (0.2 mL) were subsequently added. After 30 min, it was warmed to rt, and, 30 min later, an aliquot was taken to check the disappearance of the starting material by ^{1}H NMR. The solution was diluted to 10 mL of chloroform and washed with Na_2CO_3 sat. solution in water (20 mL) and distilled water (3 × 20 mL). The crude product was dried with Na_2SO_4, concentrated *in vacuo* and used in the following reaction without further purification.

Compound 16. To a solution of **11** (47 mg, 74 µmol), $PdCl_2(PPh_3)_2$ (5.2 mg, 7.4 µmol), PPh_3 (3.4 mg, 15.0 µmol) and CuI (1.4 mg, 7.4 µmol) in dry THF (1 mL) under N_2 atmosphere, Et_3N (1 mL) was added and three cycles of freeze-pump-thaw were performed to the mixture. TMSA (15.4 µL, 10.9 µmol) was added at rt and the temperature was increased up to 65 °C. After 12 h, the mixture was diluted in CH_2Cl_2 (15 mL), washed with water (2 × 10 mL) and brine (2 × 10 mL), dried with Na_2SO_4 and concentrated *in vacuo*. The crude product was purified by column chromatography (SiO_2, CH_2Cl_2/pentane 1:3, R_f = 0.68) to give **16** (25 mg, 53%) as an orange solid. Mp > 200 ºC; IR (neat): 2924 (m), 2855 (m), 2133 (w), 1677 (s), 1456 (m), 1380 (m), 1288 (w), 1250 (w), 1206 (s), 1143 (m), 1065 (w), 927 (w), 844 (s) 753 (w), 733 (w); ^{1}H NMR (400 MHz, $CDCl_3$): 2.81 (s, 3H), 2.45 (s, 3H), 2.40 (s, 3H), 2.38 (s, 3H), 0.29 (s, 9H); ^{13}C NMR (126 MHz, $CDCl_3$): 174.6 (q, $^2J_{C\text{-}F}$ = 36.6 Hz,

C=O), 148.2 (C), 145.5 (C), 144.3 (C), 144.1 (C), 141.4 (C), 137.8 (C), 136.6 (C), 135.1 (C), 131.1 (C), 130.9 (C), 130.7 (C), 129.7 (C), 129.3 (C), 129.3 (C), 126.3 (C), 119.6 (C), 116.7 (q, $^{1}J_{C\text{-}F}$ = 291.3 Hz, CF_3), 103.4 (C-Si), 97.6 (C), 16.9 (CH_3), 14.3 (CH_3), 14.2 (CH_3), 14.2 (CH_3), 0.1 (Si-CH_3); ^{19}F NMR (282 MHz, $CDCl_3$): -72.4; MS (APCI-): 638 (100, $[M]^-$).

Compound 17. To a solution of **14** (7.0 mg, 11 µmol) in a mixture CH_2Cl_2/MeOH (2 mL:1 mL), K_2CO_3 (5.3 mg, 39 µmol), was added. After 2 h stirring at rt, the suspension was diluted with CH_2Cl_2 (5 mL), washed with water (3 × 10 mL). The organic phase was evaporated and the crude product was used in the next step without further purification.

Compound 2. To a mixture of **17** (6.2 mg, 11 µmol), sodium 3-azidopropane-1-sulfonate (4.1 mg, 22 µmol),[S3] $CuSO_4 \cdot 5H_2O$ (2.8 mg, 11 µmol) and TBTA (0.2 mg, 0.4 µmol) in CH_2Cl_2 (2 mL), 100 µL of water and sodium ascorbate (2.2 mg, 11 µmol) were subsequently added. After 5 min, $CuSO_4 \cdot 5H_2O$ (1.4 mg, 5.5 µmol) was diluted in 200 µL of water and sodium ascorbate (1.1 mg, 5.5 µmol) was added to this solution, which was immediately poured into the reaction mixture. After 2 h under stirring at rt, the mixture was diluted with CH_2Cl_2 (5 mL) and washed with water (2 × 5 mL). The organic solvents were dried with Na_2SO_4 and evaporated *in vacuo* and the crude mixture was supported on SiO_2 and purified by column chromatography (SiO_2, CH_2Cl_2/MeOH 10:1, R_f = 0.1) to yield **2** (4.6 mg, 55%) as an orange-brown solid. NMR and IR spectroscopic data are of hydrate form. Mp: 130 – 132 ºC; IR (neat): 3320 (w), 2923 (m), 2362 (w), 1677 (s), 1372 (m), 1202 (s), 1138 (s), 1030 (s), 800 (w), 765 (w), 722 (w); ^{1}H NMR (500 MHz, DMSO-*d*$_6$ + 10% D_2O): 8.50 (s, 1H), 4.52 (t, $^{3}J_{H\text{-}H}$ = 7.1 Hz, 2H), 2.53 (m, 2H), 2.46 (s, 3H), 2.41 (s, 3H), 2.31 (m, 6H), 2.18 (p, $^{3}J_{H\text{-}H}$ = 7.1 Hz, 2H); ^{13}C NMR (126 MHz, DMSO-*d*$_6$ + 10% D_2O): 142.4 (C), 141.3 (C), 136.7 (C), 130.9 (C), 130.9 (C), 130.0 (C), 129.9 (C), 129.8 (C), 129.5 (C), 129.0 (C), 127.4 (C), 127.3 (C), 125.9 (C), 123.9 (q, $^{1}J_{C\text{-}F}$ = 288.7 Hz, CF_3), 122.3 (CH), 92.5 (q, $^{2}J_{C\text{-}F}$ = 33.2 Hz, C-$(OH)_2$), 49.3 (CH_2), 48.4 (CH_2), 26.5 (CH_2), 14.4 (CH_3), 14.2 (CH_3), 14.1 (CH_3) 14.0 (CH_3); ^{19}F NMR (282 MHz, DMSO-*d*$_6$ + 10% D_2O): -82.3; HRMS (ESI-) calcd for $C_{27}H_{19}F_3N_3O_4S_7$: 729.9378 ($[M\text{-}Na]^-$), found: 729.9387.

Compound 2'. To a mixture of **17** (6.2 mg, 11 µmol), $CuSO_4 \cdot 5H_2O$ (2.8 mg, 11 µmol) and TBTA (0.2 mg, 0.4 µmol) in 2 mL of CH_2Cl_2, 100 µL of water, 1-azidohexane[S1] (2.8 mg, 22 µmol) and sodium ascorbate (2.2 mg, 11 µmol) were subsequently added. After 5 min, $CuSO_4 \cdot 5H_2O$ (1.4 mg, 5.5 µmol) was diluted in 200 µL of water and sodium ascorbate (1.1 mg, 5.5 µmol) was added to this solution, which was immediately poured into the reaction mixture. After 2 h, the mixture was diluted with CH_2Cl_2 (5 mL) and washed with water (2 × 5 mL). The organic solvents were evaporated *in vacuo*, dried with Na_2SO_4 and the crude mixture was purified by column chromatography (SiO_2, CH_2Cl_2, R_f = 0.60) to give **5** (4 mg, 53%) as a bright orange solid. Mp: 129 – 131 ºC; IR (neat): 2923 (s), 2854 (s), 1737 (m), 1673 (m), 1458 (m), 1378 (m), 1286 (w), 1190 (m), 1144 (m), 1054 (w), 752 (w); ^{1}H NMR (400 MHz, $CDCl_3$): 7.70 (s, 1H), 4.43 (t, $^3J_{H\text{-}H}$ = 7.2 Hz, 2H), 2.81 (s, 3H), 2.57 (s, 3H), 2.41 (s, 3H), 2.39 (s, 3H), 2.02 – 1.95 (m, 2H), 1.37 – 1.34 (m, 6H), 0.92 – 0.89 (m, 3H); ^{13}C NMR (101 MHz, $CDCl_3$): 174.8 (q, $^2J_{C\text{-}F}$ = 35.7 Hz, C=O), 148.3 (C), 145.6 (C), 144.1 (C), 143.8 (C), 142.6 (C), 137.8 (C), 135.3 (C), 131.1 (C), 131.0 (C), 130.8 (C), 129.2 (C), 128.8 (C), 128.4 (C), 127.8 (C), 126.3 (C), 120.2 (CH), 116.70 (q, $^1J_{C\text{-}F}$ = 290.4 Hz, CF_3), 50.8 (CH_2), 31.3 (CH_2), 30.5 (CH_2), 26.4 (CH_2), 22.6 (CH_2), 17.0 (CH_3), 14.7 (CH_3), 14.3 (CH_3), 14.2 (CH_3), 14.1 (CH_3); ^{19}F NMR (282 MHz, $CDCl_3$): -72.4; HRMS (ESI+) calcd for $C_{30}H_{26}F_3N_3OS_6$: 694.0425 ($[M+H]^+$), found: 694.0414.

2.3. Synthesis of flippers 3 and 3'

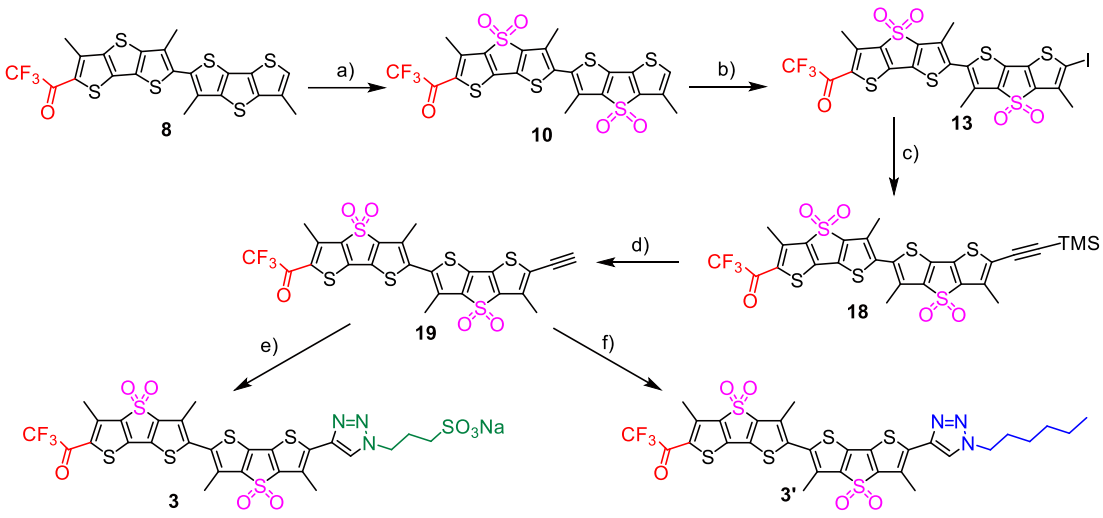

Scheme S3. (a) mCPBA, CH_2Cl_2, rt, 12 h, 40%; (b) NIS, AcOH, $CHCl_3$, rt, 0°C for 30 min, rt for 3 h; (c) TMSA, PPh_3, $PdCl_2(PPh_3)_2$, CuI, Et_3N, THF, 65 ºC, 12 h, 26%; (d) K_2CO_3, CH_2Cl_2/MeOH, rt, 2 h; (e) sodium 3-azidopropane-1-sulfonate, $CuSO_4 \cdot 5H_2O$, sodium ascorbate, TBTA, CH_2Cl_2/H_2O, rt, 2 h, 74%; (f) 1-azido hexane, $CuSO_4 \cdot 5H_2O$, sodium ascorbate, TBTA, CH_2Cl_2/H_2O, rt, 12 h, 32%.

Compound 10. To a solution of **8** (20 mg, 0.037 mmol) in CH_2Cl_2 (2 mL), mCPBA (51 mg, 0.221 mmol) was added. After 12 h under stirring at rt, the mixture was diluted with more CH_2Cl_2 (10 mL) and washed with $NaHCO_3$ sat. (3 × 10 mL) and brine (2 × 10 mL). The organic phase was dried with Na_2SO_4, filtered and evaporated *in vacuo*. Purification by column chromatography (SiO_2, CH_2Cl_2/pentane 3:1, R_f = 0.83) yielded **10** (9 mg, 40%) as an orange-brown solid. Mp: > 190 ºC; IR (neat): 2928 (m), 2852 (m), 1686 (s), 1406 (s), 1312 (s), 1212 (m), 1192 (s), (m), 1144 (s), 1104 (w), 951 (w), 752 (w), 750 (w); ^{1}H NMR (400 MHz, $CDCl_3$): 7.00 (s, 1H), 2.81 (s, 3H), 2.46 (s, 3H), 2.43 (s, 3H), 2.40 (s, 3H); ^{13}C NMR (126 MHz, $CDCl_3$): 173.6 (q, $^2J_{C\text{-}F}$ = 37.9 Hz, C=O), 146.2 (C), 144.0 (C), 143.4 (C), 142.9 (C), 142.3 (C), 136.9 (C), 136.1 (C), 135.1 (C), 133.9 (C), 133.6 (C), 133.2 (C),

130.1 (C), 129.8 (C), 128.5 (C), 126.5 (CH), 116.1 (q, $^{1}J_{C\text{-}F}$ = 290.8 Hz, CF_3), 15.1 (CH_3), 13.3 (CH_3), 12.6 (CH_3), 12.5 (CH_3); ^{19}F NMR (282 MHz, $CDCl_3$): -73.1; MS (APCI-): 606 (100, $[M]^-$).

Compound 13. To a solution of **10** (20 mg, 0.033 mmol) in chloroform (2 mL) at 0 °C, NIS (30 mg, 0.50 mmol) and AcOH (0.1 mL) were subsequently added. After 30 min, it was warmed to rt and, 3 h later, an aliquot was taken, checking the disappearance of the starting material. The solution was diluted to 10 mL of chloroform and washed with Na_2CO_3 sat. solution in water (20 mL) and distilled water (3 × 20 mL). This crude product was dried with Na_2SO_4, concentrated *in vacuo* and used in the following reaction without further purification.

Compound 18. To a solution of **13** (21 mg, 33 µmol), $PdCl_2(PPh_3)_2$ (2.3 mg, 3.3 µmol), PPh_3 (1.5 mg, 6.6 µmol) and CuI (0.7 mg, 3 µmol) in dry THF (0.4 mL) under N_2 atmosphere, Et_3N (0.4 mL) was added and three cycles of freeze-pump-thaw were performed to the mixture. TMSA (7 µL, 5 µmol) was added at rt and the temperature was increased up to 65 °C. After 12 h, the mixture was diluted in CH_2Cl_2 (10 mL), washed with water (2 × 7 mL) and brine (2 × 7 mL), dried with Na_2SO_4 and concentrated *in vacuo*. The crude product was purified by column chromatography (SiO_2, CH_2Cl_2/pentane 3:1, R_f = 0.62) to give **18** (6 mg, 26%) as an orange solid. Mp > 180 ºC; IR (neat): 2922 (s), 2853 (s), 1735 (m), 1489 (w)), 1463 (m), 1378 (m), 1314 (m), 1289 (s), 1146 (m), 966 (w), 857 (m), 844 (s), 752 (w), 722 (w); ^{1}H NMR (400 MHz, $CDCl_3$): 2.81 (s, 3H), 2.47 (m, 3H), 2.43 (s, 3H), 2.40 (s, 3H), 0.29 (s, 9H); ^{13}C NMR (126 MHz, $CDCl_3$): 173.6 (q, $^{2}J_{C\text{-}F}$ = 38.8 Hz, C=O), 146.3 (C), 146.2 (C), 144.1 (C), 143.9 (C), 142.2 (C), 137.9 (C), 136.6 (C), 135.9 (C), 133.9 (C), 133.4 (C), 132.9 (C), 130.5 (C), 130.1 (C), 125.0 (C), 116.1 (q, $^{1}J_{C\text{-}F}$ = 290.5 Hz, CF_3), 107.3 (C-Si), 95.0 (C), 15.1 (CH_3), 12.7 (CH_3), 12.6 (CH_3), 12.6 (CH_3), -0.1 (Si-CH_3); ^{19}F NMR (282 MHz, $CDCl_3$): -73.1; MS (APCI-): 702 (100, $[M]^-$).

Compound 19. To a solution of **18** (4.0 mg, 5.7 µmol) in a mixture CH_2Cl_2/MeOH (2 mL:1 mL), K_2CO_3 (2.8 mg, 20.3 µmol), was added. After 2 h stirring at rt, the suspension was diluted with

CH_2Cl_2 (5 mL), washed with water (3 × 10 mL) and concentrated *in vacuo*. The organic phase was evaporated and the crude product was used in the next step without further purification.

Compound 3. To a mixture of **19** (3.0 mg, 4.3 µmol), sodium 3-azidopropane-1-sulfonate (1.6 mg, 8.6 µmol),[S3] $CuSO_4 \cdot 5H_2O$ (1.1 mg, 4.3 µmol) and TBTA (0.1 mg, 0.5 µmol) in CH_2Cl_2 (1 mL), 200 µL of water and sodium ascorbate (0.9 mg, 4.3 µmol) were subsequently added. After 5 min, $CuSO_4 \cdot 5H_2O$ (0.6 mg, 2.2 µmol) was diluted in 200 µL of water and sodium ascorbate (0.5 mg, 0.6 µmol) was added to this solution, which was immediately poured into the reaction mixture. After 2 h under stirring, the mixture was diluted with CH_2Cl_2 (5 mL) and washed with water (2 × 5 mL). The organic solvents were evaporated *in vacuo* and the crude mixture was supported on SiO_2 and purified by column chromatography (SiO_2, CH_2Cl_2/MeOH 6:1, R_f = 0.2) to yield **3** (2.6 mg, 74%) as an orange-brown solid. NMR and IR spectroscopic data are of hydrate form. Mp: decomp. > 170 ºC; IR (neat): 3305 (br), 2921 (m), 1682 (m), 1396 (m), 1306 (s), 1182 (s), 1144 (s), 1053 (s), 752 (m); ^{1}H NMR (500 MHz, DMSO-*d*$_6$ + 10% D_2O): 8.49 (s, 1H), 4.51 (t, $^3J_{H\text{-}H}$ = 7.1 Hz, 2H), 2.53 (t, $^3J_{H\text{-}H}$ = 7.1 Hz, 2H), 2.41 (s, 3H), 2.36 (s, 3H), 2.25 (s, 6H), 2.17 (p, $^3J_{H\text{-}H}$ = 7.1 Hz, 2H); ^{13}C NMR (126 MHz, DMSO-*d*$_6$ + 10% D_2O): 142.6 (C), 142.3 (C), 142.1 (C), 141.8 (C), 141.6 (C), 139.7 (C), 136.2 (C), 135.7 (C), 134.7 (C), 134.4 (C), 132.9 (C), 132.8 (C), 132.3 (C), 132.2 (C), 131.7 (C), 128.0 (C), 123.3 (q, $^1J_{C\text{-}F}$ = 293.1 Hz, CF_3), 122.9 (CH), 92.2 (m, C-$(OH)_2$), 49.4 (CH_2), 48.2 (CH_2), 26.2 (CH_2), 12.6 (CH_3), 12.2 (CH_3), 12.1 (CH_3); ^{19}F NMR (282 MHz, DMSO-*d*$_6$ + 10% D_2O): -84.1; HRMS (ESI-) calcd for $C_{27}H_{19}F_3N_3NaO_8S_7$: 793.9174 ($[M\text{-}Na]^-$), found: 793.9180.

Compound 3'. To a mixture of **19** (3.6 mg, 5.7 µmol), $CuSO_4 \cdot 5H_2O$ (1.5 mg, 5.7 µmol) and TBTA (0.1 mg, 0.2 µmol) in 2 mL of CH_2Cl_2, 100 µL of water, 1-azidohexane (3.0 mg, 24 µmol) and sodium ascorbate (1.2 mg, 5.7 µmol) were subsequently added. After 5 min, $CuSO_4 \cdot 5H_2O$ (0.8 mg, 3 µmol) was diluted in 200 µL of water and sodium ascorbate (0.6 mg, 3 µmol) was added to this solution, which was immediately poured into the reaction mixture. After 2 h, the mixture was diluted with CH_2Cl_2 (5 mL) and washed with water (2 × 5 mL). The organic solvents were evaporated *in*

vacuo and the crude mixture was purified by column chromatography (SiO_2, CH_2Cl_2, R_f = 0.05) to give **3'** (1.4 mg, 32%) as a dark orange solid. Mp > 190 ºC; IR (neat): 2924 (s), 2854 (s), 1682 (m), 1397 (m), 1312 (m), 1193 (m), 1145 (s), 753 (w); ^{1}H NMR (500 MHz, $CDCl_3$): 7.71 (s, 1H), 4.44 (t, $^3J_{H\text{-}H}$ = 7.3 Hz, 2H), 2.81 (s, 3H), 2.56 (s, 3H), 2.44 (s, 3H), 2.41 (s, 3H), 1.99– 1.96 (m, 2H), 1.36 – 1.34 (m, 6H), 0.91 – 0.89 (m, 3H); ^{13}C NMR (126 MHz, $CDCl_3$): 173.6 (q, $^2J_{C\text{-}F}$ = 37.5 Hz, C=O), 146.3 (C), 146.2 (C), 144.1 (C), 143.7 (C), 142.8 (C), 142.3 (C), 140.7 (C), 136.9 (C), 136.1 (C), 134.5 (C), 133.9 (C), 133.8 (C), 133.2 (C), 132.6 (C), 130.1 (C), 130.1 (C), 128.7 (C), 120.2 (CH), 116.1 (q, $^1J_{C\text{-}F}$ = 291.0 Hz, CF_3), 51.0 (CH_2), 31.3 (CH_2), 30.4 (CH_2), 26.3 (CH_2), 22.6 (CH_2), 15.1 (CH_3), 14.1 (CH_3), 13.1 (CH_3), 12.6 (CH_3), 12.6 (CH_3); ^{19}F NMR (282 MHz, $CDCl_3$): -73.1; HRMS (MeOH hemiacetal, ESI+) calcd for $C_{31}H_{30}F_3N_3O_6S_6$: 790.0485 ($[M+H]^+$), found: 790.0478.

3. Solvatochromism

The absorption and fluorescence emission spectra (λ_{ex} = 425 nm) of **2**, **2'**, **3** and **3'** were recorded at 25 ºC in solvents of different polarity (*c* (**2, 3**) = 3 µM; *c* (**2'**) = 1 µM; *c* (**3'**) = 0.7 µM). The absorbance of the solutions was < 0.1.

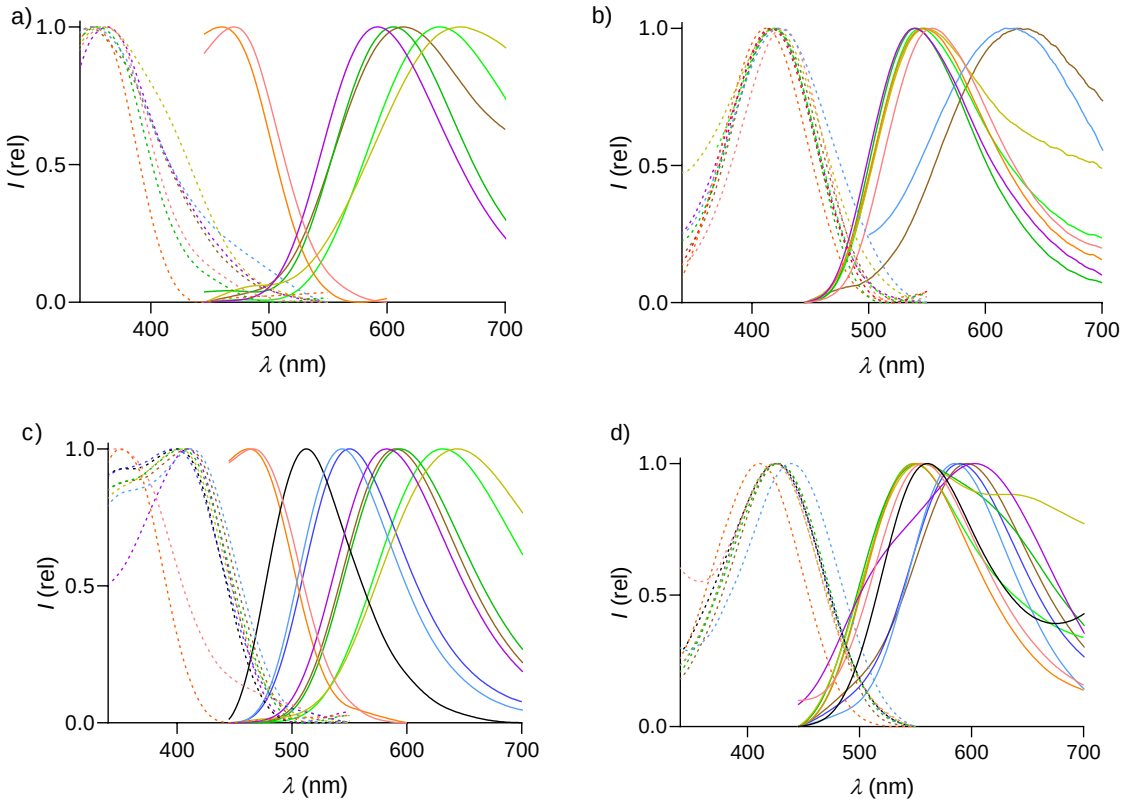

Fig. S2 Normalized absorption (dashed) and emission spectra (solid, λ_{ex} = 425 nm) of (a) **2**, (b) **3**, (c) **2'** and (d) **3'**; in DMSO (red), MeCN (dark yellow), MeOH (orange), $CHCl_3$ (brown), acetone (light green), THF (dark green), EtOAc (purple), toluene (light blue), Et_2O (dark blue) and cyclohexane (black).

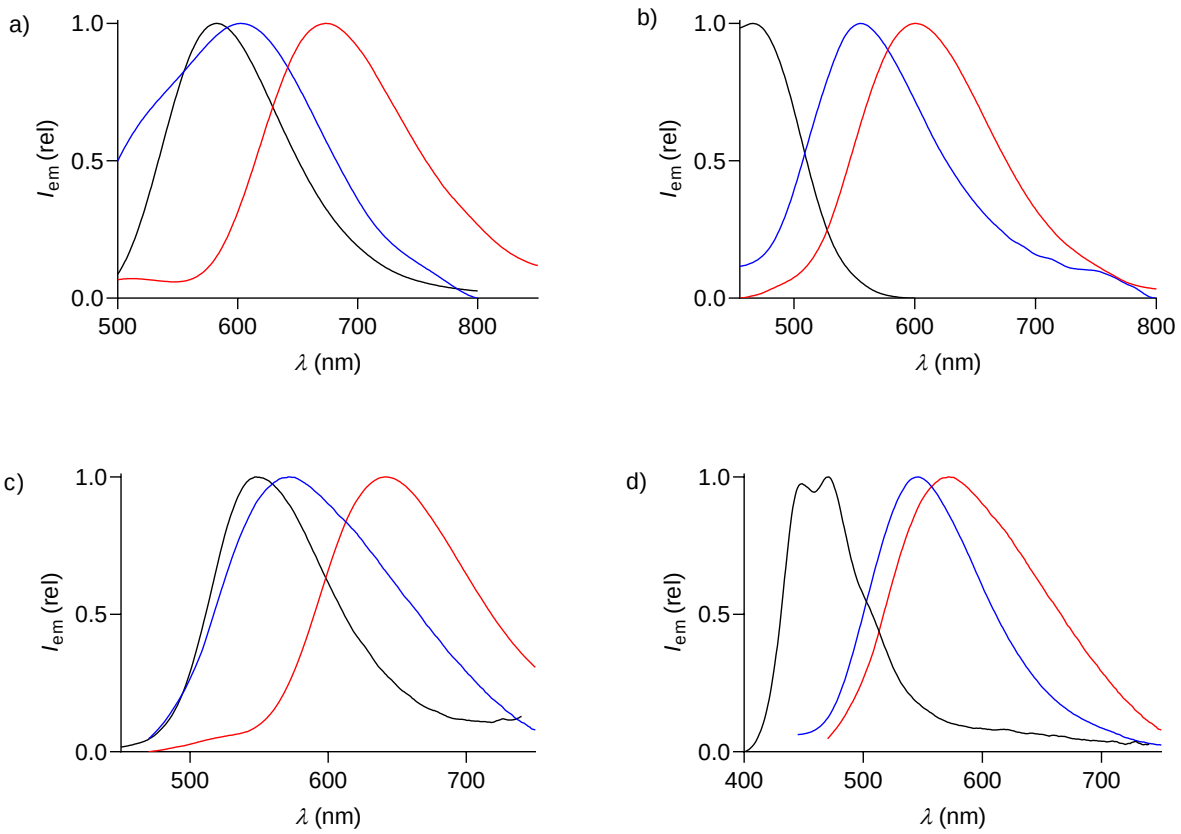

Fig. S3 Normalized emission spectra (λ_{ex} = 425 nm) of **1'** (red), **2'** (black) and **3'** (blue) in (a) EtOAc "ketone" (b) DMSO "hydrate" (c) dioxane "ketone" and (d) dioxane:water solutions **1**' (20:1), **2**' (50:50) and **3** (10:1) "hydrate".

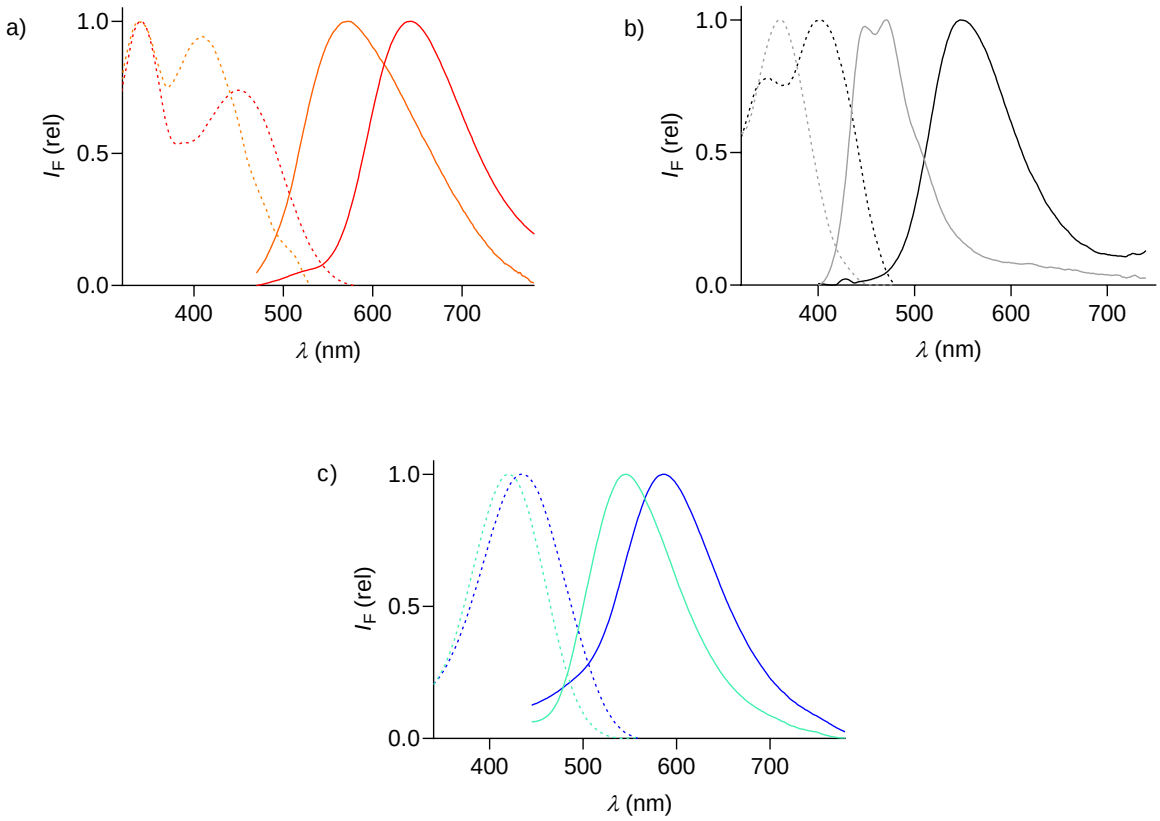

Fig. S4 Normalized emission (plain) and excitation (dotted) spectra in dioxane (red – black – blue) and in dioxane:water (orange 20:1 – grey 50:50 – cyan 10:1) of (a) **1'**, λ_{ex} = 435 nm, λ_{em} = 600 nm; (b) **2'**, λ_{ex} = 380 nm, λ_{em} = 540 nm and (c) **3'**, λ_{ex} = 425 nm, λ_{em} = 580 nm.

Lippert-Mataga plots. As in ref S1. A comparison of the solvatochromic response in function of the properties of the solvents was performed by the Lippert-Mataga equations, with Scholte's modification.[S4] The difference in wavenumber ($\Delta\nu = \nu_a - \nu_b$) of the absorption maximum ν_a and that of emission maximum ν_b in each solvent, were plotted against $f(\varepsilon)$-$f(n)$ and linearly correlated (Equation (S1), Fig. S5).

$$\nu_a - \nu_b = g\frac{f(\varepsilon)-f(n)}{hc}\Delta\mu^2 + const. \quad \text{(S1)}$$

$$g = \frac{3}{abd} \quad \text{(S2)}$$

$$f(\varepsilon) = \frac{A_1(1-A_1)(\varepsilon-1)}{\varepsilon+(1-\varepsilon)A_1} \quad \text{(S3)}$$

$$f(n) = \frac{A_1(1-A_1)(n^2-1)}{n^2+(1-n^2)A_1} \quad \text{(S4)}$$

$$A_1 = \frac{-1}{p^2-1} + \frac{p}{\sqrt{p^2-1}^3}\ln\left(p+\sqrt{p^2-1}\right) \quad \text{(S5)}$$

$$p = \frac{a}{b} \quad \text{(S6)}$$

where *a*, *b*, and *d* (*a* > *b* = *d*) (cm) are the prolate dimensions, *n* refractive indexes, ε solvent dielectric constant, ν_a and ν_b (cm^{-1}) are the absorption and emission wavenumbers of the maximum of intensity for each fluorophore in each solvent, *h* (erg) is the Planck constant, *c* ($cm \cdot s^{-1}$) is the light speed and $\Delta\mu$ the variation of dipole moment upon excitation. Dimension *a* was considered as half of the distance between N of the triazol donor and O from the CO acceptor, estimated from an optimization of the structure in Chem3D, ChembioDraw software. From the same calculations dimension *b* = *d* was estimated as half of the diameter of the smallest hypothetical cylinder in which the fluorophore would fit.

It was not possible to make a reliable linear regression fit for **2** or **3**; as it happened for **1**,[S1] it is likely to be related to the low solubility and formation of the hemiacetal/diol of the compounds in some of the solvents. **1'** and **3'** presented more similar responses because of the ketone/hydrate equilibrium. Therefore, as it was previously reported for **1'**, [S1] for the Lippert-Mattaga plots (Fig. S5), compound **3'** in methanol, or solvents containing water, were not taken into account for the fitting, being extremely sensitive to hydration or formation of the hemiacetal (see section 5)

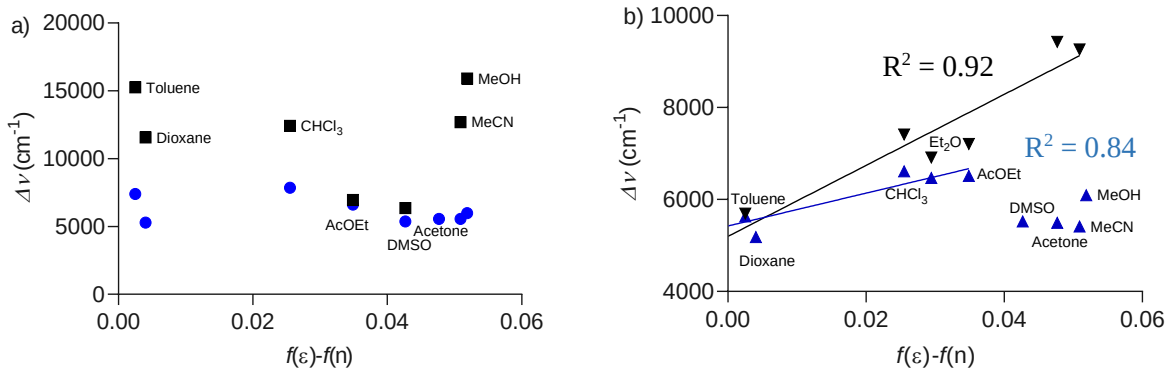

Fig. S5 Lippert-Mataga plots for the compounds (a) **2** (black), **3** (blue) and (b) **2'** (black) and **3'** (blue); linearly fitted to the equation S1.

Table S1 Linear fit parameters and transition dipole moments.

Entry	Cpd[a]	*a* (Å)[b]	*b* = *d* (Å)[c]	$g\Delta\mu^2/hc$[d]	*Const*[e]	$\Delta\mu$ (D)[f]
1	**1'**[g]	8.35	2.45	54659 ± 5521	5720 ± 167	13.5 ± 0.7
2	**2'**	8.35	2.45	77184 ± 10192	5197 ± 336	16.0 ± 1.0
3	**3'**	8.35	2.45	35773 ± 7691	5422 ± 165	10.9 ± 1.1

[a]Compounds **1' – 3'**. [b]Prolate dimension "a". [c] Prolate dimension "b". [d]Slope of the fits to equation (S1) from Fig. S5. [e]Intercept of fits in Fig. S5. [f]Variation in dipole moments calculated according to equations (S1) – (S6). [g]Data from reference S1.

4. Fluorescence quantum yields

Fluorescence quantum yields were calculated for solutions with absorbance < 0.1. They were evaluated based on a standard, whether quinine sulfate (H_2SO_4 0.1 M in water, Φ_R = 51 %, λ_{ex} = 350 nm) or fluorescein (EtOH, λ_{ex} = 410 nm, Φ_R = 79%), using equation (S7):

$$\Phi = \Phi_R \frac{Int}{Int_R}\left(\frac{OD_R}{OD}\right)\frac{n^2}{n_R^2} \quad \text{(S7)}$$

$$OD = 1 - 10^{-A} \quad \text{(S8)}$$

Φ_R is the quantum yield of the standards, *Int* is the area of the emission intensity of the sample, Int_R is the area of the emission intensity of the standard, *A* is the absorbance, A_R is the absorbance of the standard, *OD* is the optical density of the sample, OD_R is the optical density of the standard, *n* is the refractive index of the sample and n_R is the refractive index of the standard.

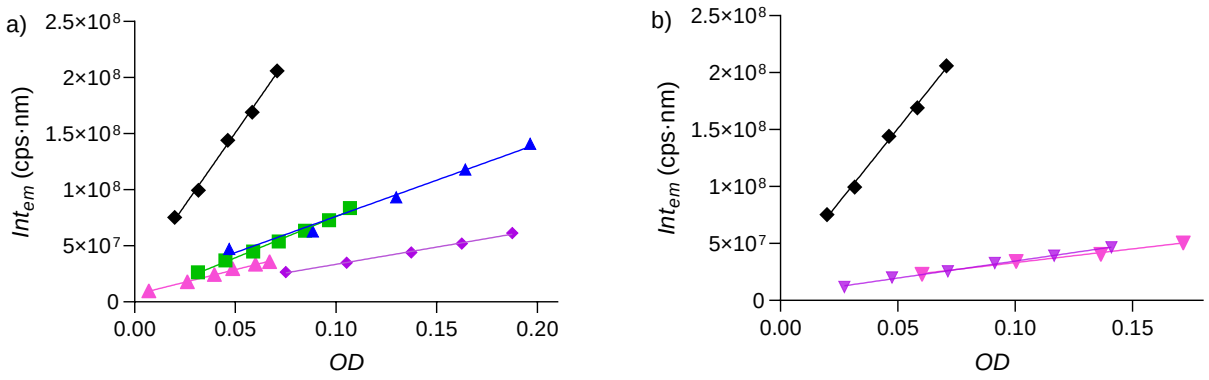

Fig. S6 *OD* against integral of the emission between 450 – 750 nm. (a) Fluorescein (black, Φ_R = 79%, EtOH), **2** (green, Φ = 25%, dioxane), **3** (pink, Φ = 7%, dioxane), **2'** (blue, 22%, dioxane) and **3'** (purple, Φ = 10%, dioxane). (b) Fluorescein (black, Φ_R = 79%, EtOH), **3** (pink, Φ = 8%, dioxane/water 9:1) and **3'** (purple, Φ = 10%, dioxane/water 9:1).

Molar extinction coefficients. From the solutions in dioxane or dioxane:water mixtures that were measured for calculating the fluorescence quantum yield of each probe, the molar extinction

coefficients were also calculated and expressed as the average of the different absorbance / concentration, the error was calculated from a t-student test with a confidence interval of 95 %.

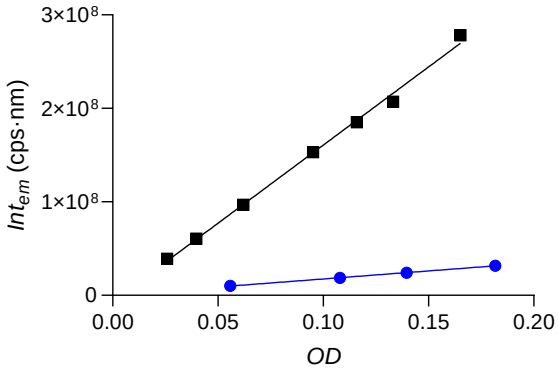

Fig. S7 *OD* against integral of the emission between 370 – 750 nm of quinine sulfate in H_2SO_4 0.1 M water solution (black, Φ_R = 51 %) and **2'** in dioxane/water, 50:50 (blue, Φ = 6%).

Table S2 Molar extinction coefficient at the relative maxima of absorption.

Entry	Cpd[a]	ε ($mM^{-1}cm^{-1}$)[b]				
		350 nm	450 nm	425 nm	440 nm	460 nm
1	**1'**[c]	50.6 ± 1.2	27.9 ± 0.7	-	-	37.1 ± 0.7
2	**1'w**[d]	45.0 ± 1.5	33.9 ± 1.5	-	-	10.2 ± 1.3
3	**2'**[c]	39.9 ± 1.3	46.6 ± 1.5	-	-	-
4	**2'w**[e]	41.1 ± 2.7	41.6 ± 3.1	-	-	-
5	**3'**[c]	-	-	-	31.8 ± 1.9	-
6	**3'w**[f]	-	-	22.8 ± 0.4	-	-

[a]Compounds. [b]Molar extinction coefficient. [c]In dioxane. [d]Dioxane/water 20:1. [e]Dioxane/water 50:50. [f]Dioxane/water 10:1.

5. Dynamic-covalent ketone chemistry

Kinetics of hydrate formation. 1 μM solutions of **1'**, **2'** and **3'** were prepared in dioxane and water (1.25 M) was added. The effect over fluorescence for the formation of the diol was studied against time; 25 ºC were maintained for all the experiments. The equation for the kinetic was fitted to a first order exponential:

$$I = -(1 - e^{kt})(I_0 - I_p) + I_0 \quad \text{(S9)}$$

$$t_{1/2} = 1/k \quad \text{(S10)}$$

where I is the intensity or intensity ratio change at specific wavelengths, I_p is its value at the plateau, I_0 is its initial value, t is the time in hours and $t_{1/2}$ is the half life.

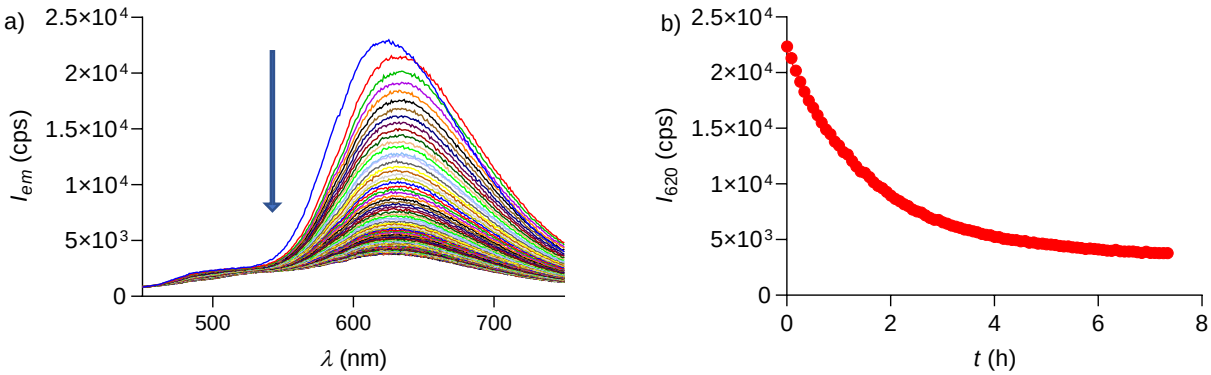

Fig. S8 Intensity of fluorescence against time, response of **1'** (a) emission spectra, (λ_{ex} = 450 nm) and (b) emission intensity at 620 nm against time. Calculated $t_{1/2}$ = 1.61 h.

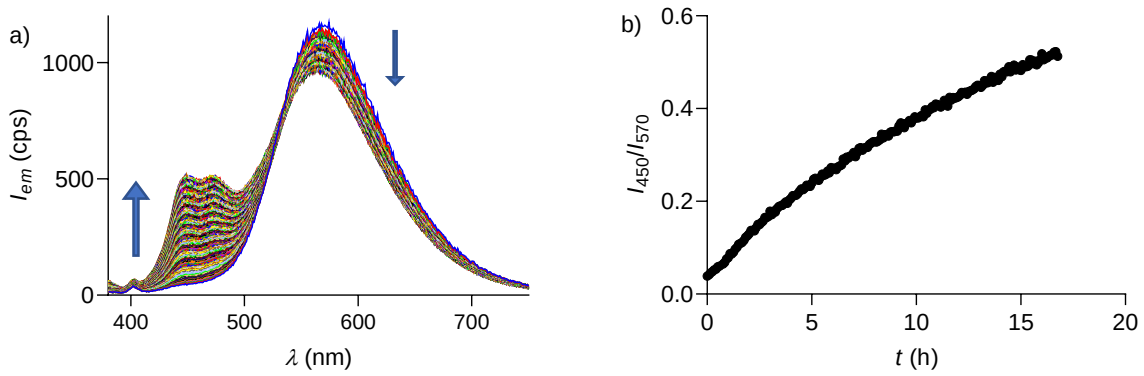

Fig. S9 Intensity of fluorescence against time, response of **2'** (a) emission spectra (λ_{ex} = 350 nm) and (b) ratio of hydrate/ketone (I_{450}/I_{570}). Calculated $t_{1/2}$ > 16.1 h.

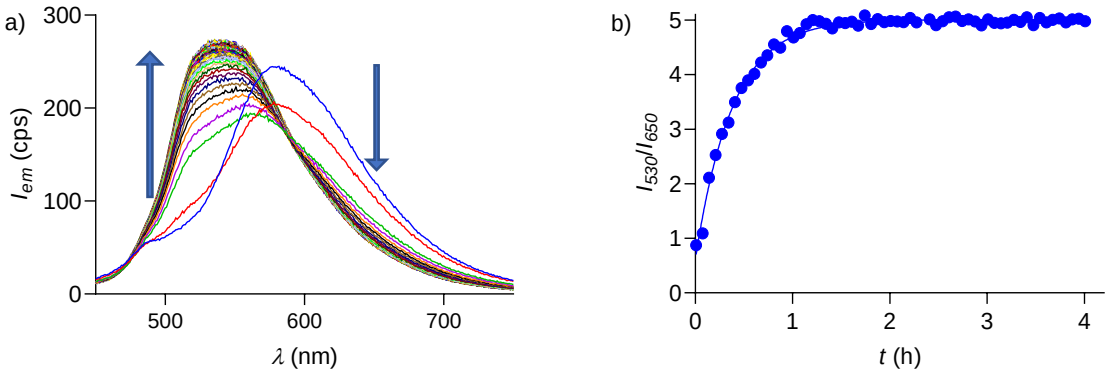

Fig. S10 Intensity of fluorescence against time, response of **3'** (a) emission spectra (λ_{ex} = 350 nm) and (b) ratio of hydrate/ketone (I_{530}/I_{650}). Calculated $t_{1/2}$ = 0.38 h.

Water concentration dependence. Solutions of **2'** and **3'** were prepared in dioxane (1 µM) and different concentrations of water were added. The effect over fluorescence for the formation of the diol was studied against concentration of water by preparing the solutions and measuring after 48 hours; 25 ºC and 2 nm excitation and emission slits were used for all the experiments. In order provide

an EC_{50} value for the concentration needed to have 50% diol/ketone the changes were fitted to the Hill equation:

$$I = I_0 + c^n \frac{I_p - I_0}{c^n + EC_{50}^n} \quad \text{(S11)}$$

where I is the intensity or intensity ratio change at specific wavelengths, I_p is its value at the plateau, I_0 is its initial value, EC_{50} is the concentration associated to the middle point between I_p and I_0 (50% diol/ketone) and n is the Hill slope.

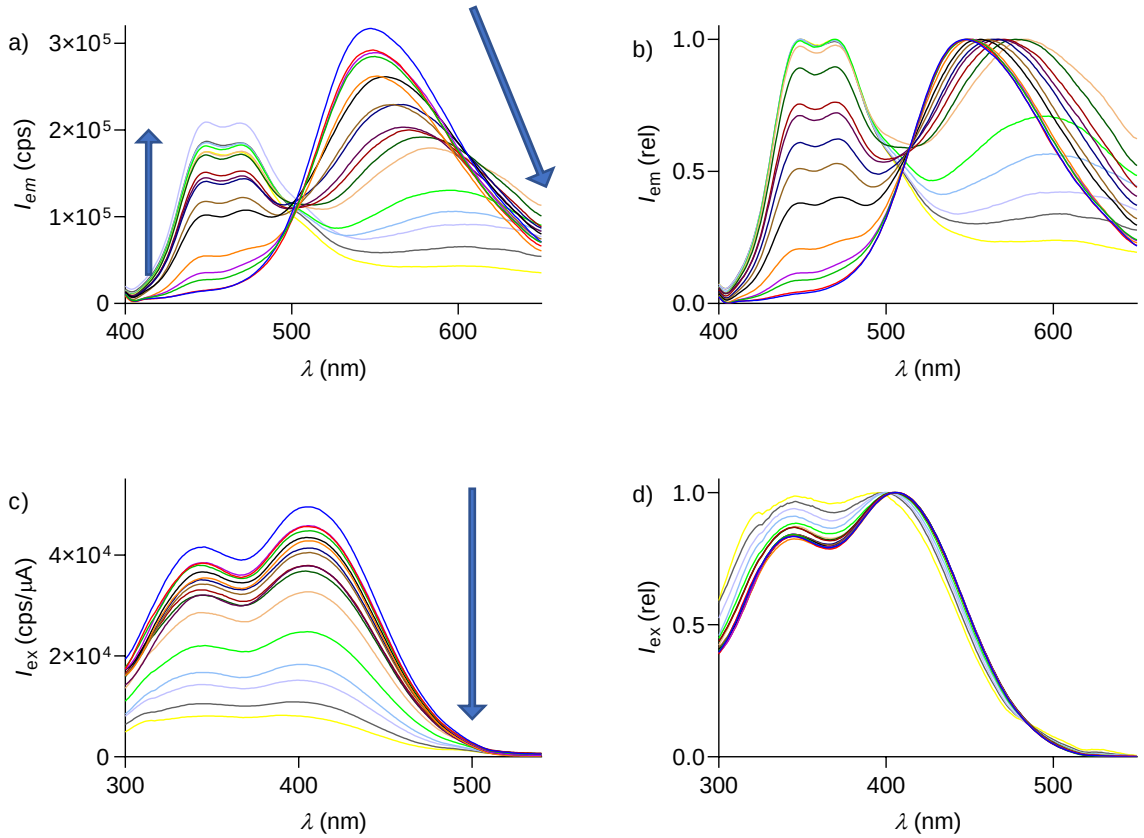

Fig. S11 Spectroscopic response of **2'** in dioxane (1 µM) with increasing concentrations of water from 0 to 10 M (a) emission spectra (λ_{ex} = 350 nm); (b) normalized emission spectra (λ_{ex} = 350 nm); (c) excitation spectra (λ_{em} = 580 nm) and (d) normalized excitation spectra (λ_{em} = 580 nm).

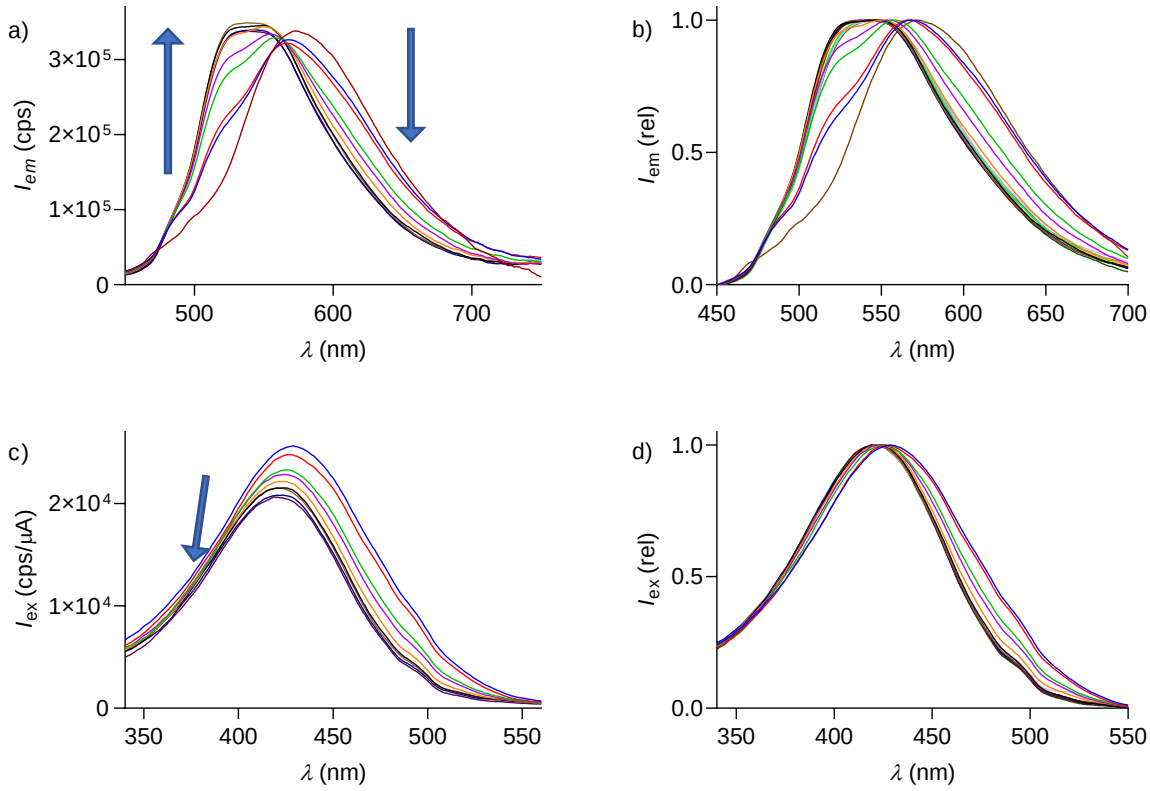

Fig. S12 Spectroscopic response of **3'** in dioxane (1 μM) with increasing concentrations of water from 0 to 10 M (a) emission spectra (λ_{ex} = 425 nm); (b) normalized emission spectra (λ_{ex} = 425 nm); (c) excitation spectra (λ_{em} = 580 nm) and (d) normalized excitation spectra (λ_{em} = 580 nm).

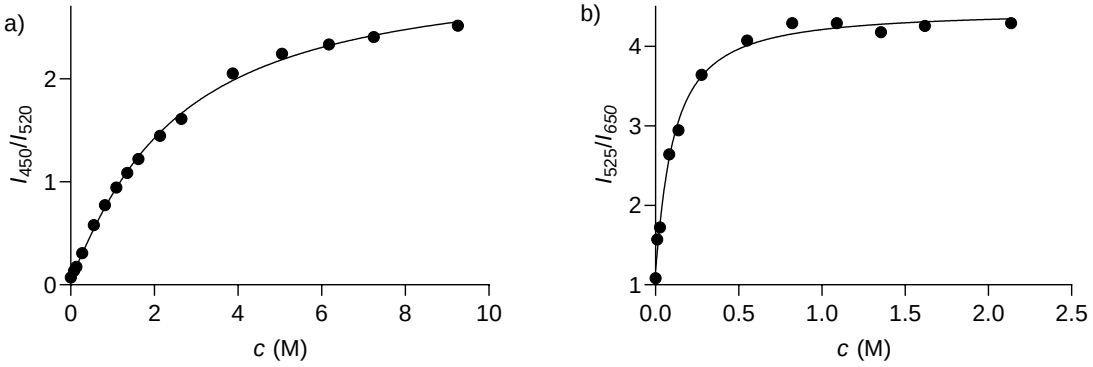

Fig. S13 Emission intensity ratio against water concentration in dioxane fitted to equation S11 (a) **2'** (λ_{ex} = 350 nm, 1 μM, emission intensity ratio I_{450}/I_{520}, EC_{50} = 2.4 ± 0.2 M, n = 1.2 ± 0.1) and (b) **3'** in dioxane (λ_{ex} = 425 nm, 1 μM, emission intensity ratio I_{525}/I_{650}, EC_{50} = 106 ± 12 mM, n = 1.1 ± 0.2).

6. Fluorescence spectroscopy in LUVs

Large unilamellar vesicles (LUVs) stock solutions were prepared according to previously reported procedures.[S5]

DOPC (1,2-dioleoyl-sn-glycero-3-phosphocholine) LUVs. As described in S1; a lipid film was prepared by evaporating a solution of DOPC (23 mg) in MeOH/$CHCl_3$ 1:9 (1 mL), then the flask was put under vacuum overnight. The resulting film was hydrated with a buffer solution (1.0 mL, 10 mM Tris, 100 mM NaCl, pH 7.4) for 30 min at rt, subjected to freeze-thaw cycles (10×, liquid N_2, 55 °C water bath) and extruded (15×) through a polycarbonate membrane (pore size, 100 nm) using a Mini-extruder.

SM/CL (sphingomyelin/cholesterol) LUVs were prepared similarly using SM (14.8 mg) and CL (3.5 mg). Hydration (with 1 mL of the buffer) and extrusion were performed at 65 ºC.

Fluorescence spectroscopy in LUVs, general procedure. 5 nm slits were used for both excitation and emission. To a buffer solution (2.0 mL, 10 mM Tris, 100 mM NaCl, pH 7.4) at 25 °C

in a quartz cuvette were added LUVs (5 µL of 30 mM lipid, 75 µM). The probe (between 2 to 20 µL of a stock solution in DMSO of the corresponding concentration) was added and the emission and excitation spectra were recorded. The same solutions without probe served as backgrounds.

Concentration dependence in LUVs. Under the conditions explained in the general procedure, the concentration of probe was increased using 10 or 100 µM stock solutions in DMSO, and the increase in fluorescence **2** (λ_{em} = 580 nm) and **3** (λ_{em} = 550 nm) was recorded 1 h after each addition. Probe **3** presented low partitioning / higher fluorescence in buffer solution than in the DOPC or SM/CL (see Fig. S18c) and probes **2'** and **3'** did not partition in LUVs.

Partition kinetics. Following the general procedure, 2 µL of **1** and **2** (100 µM, DMSO) were added and the increase in fluorescence was followed against time, λ_{em} = 580 nm.

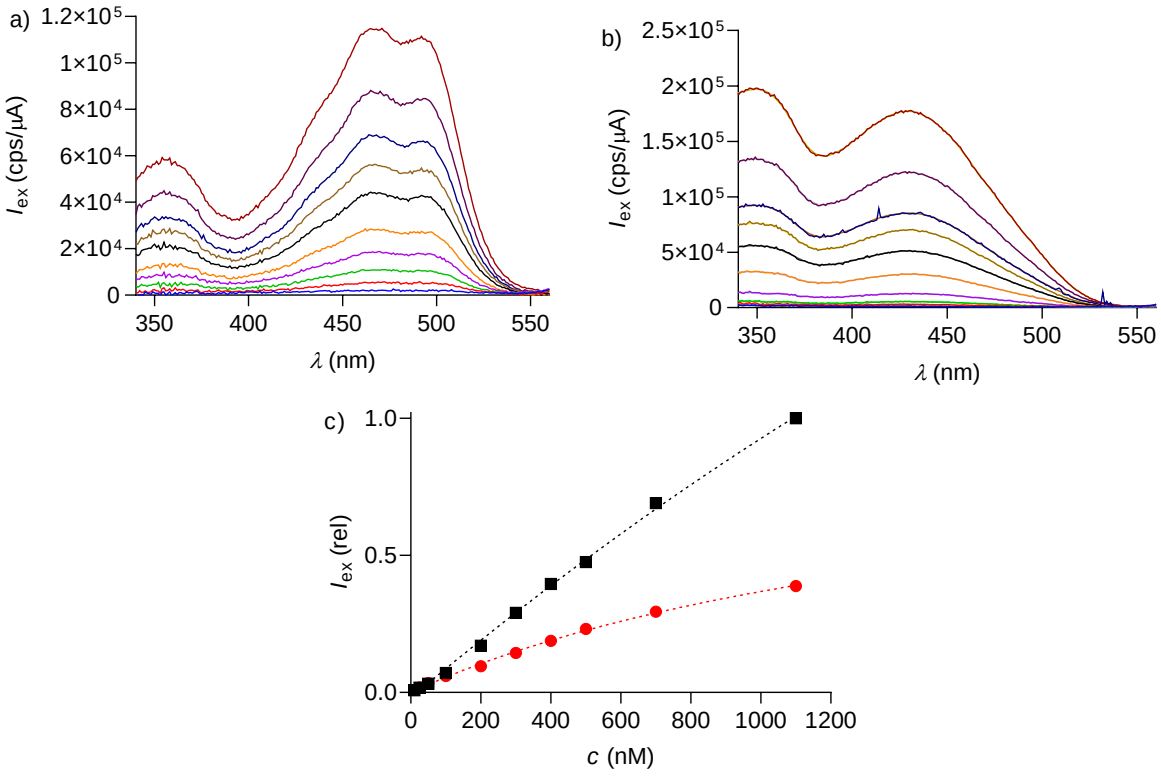

Fig. S14 Concentration dependence of **2** (λ_{em} = 580 nm) in (a) SM/CL LUVs, (b) DOPC LUVs, (c) intensity at 430 nm against concentration of the probe in DOPC (black) and in SM/CL (red) LUVs.

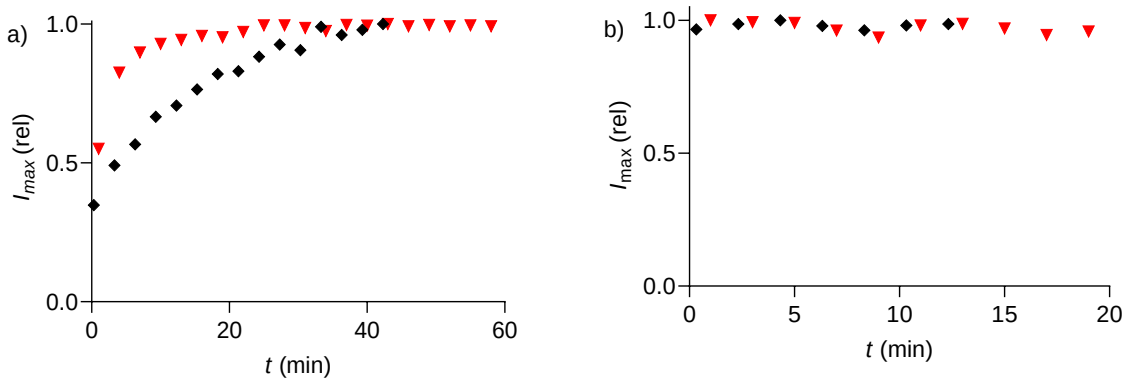

Fig. S15 Maximum of excitation intensity (intensity/max. intensity) against time, 100 nM solutions of **1** (red, λ_{em} = 600 nm) and **2** (black, λ_{em} = 580 nm), (a) SM/CL and (b) DOPC LUVs.

Analysis of excitation and emission spectra. As in S1, the contribution of different electronic transitions was estimated for the excitation spectra in SM/CL LUVs by fitting to Gaussian functions using the software fityk. Three Gaussian functions were needed to satisfactorily fit the highly structured low energy band. The gaussian peaks with lowest and middle energy would correspond to the 0-0 and 0-1 transitions respectively. However, the one with highest energy seems to report on how well the probes partition to the membrane, where a broad band and/or a blueshift would happen if the partitioning is not ideal. Therefore, the one with the lowest energy level was taken for comparisons as it was performed in previous studies.[S5]

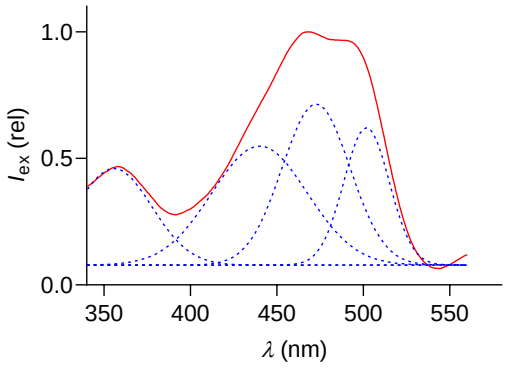

Fig. S16 Deconvolution of the excitation spectra of **2** (λ_{em} = 580 nm, 100 nM) in SM/CL LUVs.

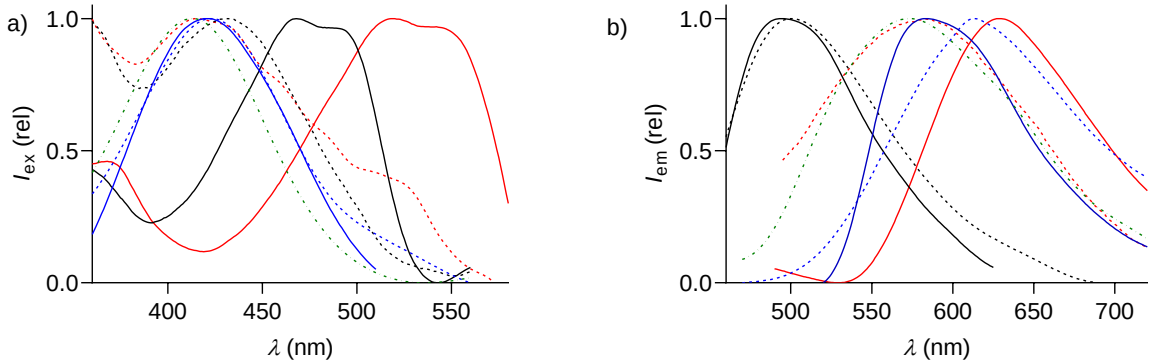

Fig. S17 Normalized (a) excitation and (b) emission spectra of probes **1** (red, λ_{em} = 600 nm, λ_{ex} = 430 nm), **2** (black, λ_{em} = 560 nm, λ_{ex} = 425 nm) and **3** (blue, λ_{em} = 580 nm, λ_{ex} = 450 nm); 100 nM probes in SM/CL LUVs (solid), in DOPC LUVs (dashed) and in TRIS buffer solution pH 7.4 (**3**, green dotted).

Table S3 Excitation spectra in LUVs, calculated parameters

Entry	Cpd[a]	λ_{Lo^E} (nm)[b]	$\lambda_{Lo^{01}}$ (nm)[c]	$\lambda_{Lo^{00}}$ (nm)[d]	λ_{Ld} (nm)[e]	$\Delta\lambda_{(Lo - Ld)}$ (nm)[f]	I_{Lo}/I_{Ld}[g]
1	**1**[i]	492	526	560	418	142[h]	8
2	**2**	440	472	502	432	70	1.4
3	**3**	-	-	422	422	0	0.2

[a]Compounds **1** – **3**. [b]Wavelength of the maximum for the Gaussian function with the third lowest energy in SM/CL LUVs. [c]Wavelength of the maximum for the Gaussian function with the second lowest energy, 0-1 transition in SM/CL LUVs. [d]Wavelength of the maximum for the Gaussian function with the lowest energy, 0-0 transition in SM/CL LUVs. [e]Wavelength of the maximum in DOPC LUVs. [f]Difference in the wavelength of the lowest energy excitation maxima, SM/CL ($\lambda_{Lo^{00}}$) - DOPC (λ_{Ld}) LUVs. [g]Intensity ratio of the lowest energy excitation maxima, SM/CL ($I_{Lo^{00}}$) / DOPC (I_{Ld}) LUVs. [h]Probe **1** in DOPC LUVs at 25 ºC presented very low fluorescent emission associated to the formation of the hydrate. [i]As reported in S1.

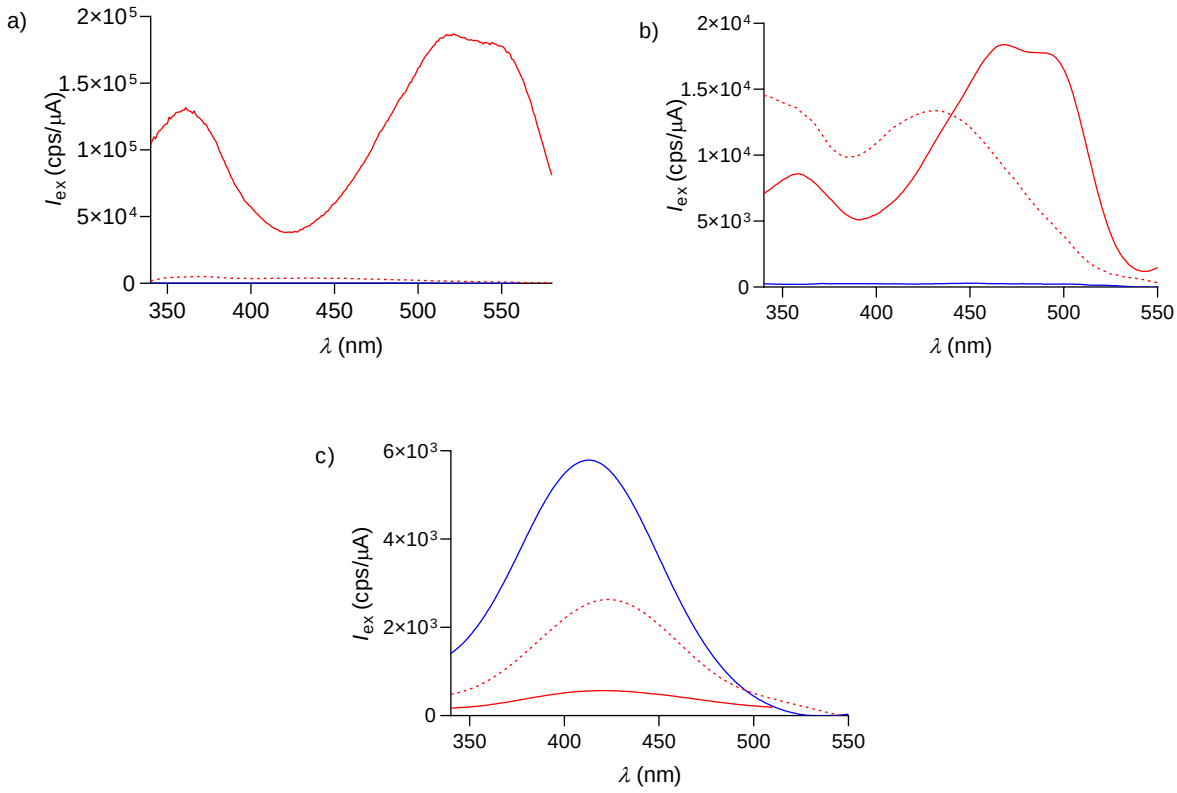

Fig. S18 Excitation spectra in SM/CL LUVs (solid red), DOPC LUVs (dashed red) and without LUVs (solid blue) of (a) **1** (100 nM, λ_{em} = 600 nm), (b) **2** (100 nM, λ_{em} = 580 nm) and (c) **3** (100 nM, λ_{em} = 580 nm).

Partition coefficients.[S6] From a concentrated DOPC or SM/CL LUVs stock solution, increasing volumes were added to a 2 mL buffer solution (Tris 10 mM, NaCl 100 mM, pH 7.4) containing the different probes (100 nM) and thermostated at 25 °C. The emission spectra were acquired with slit 5:2 for SM/CL LUVs and 5:5 for DOPC LUVs, 15 min after every LUVs addition, when the equilibrium was reached. K_x values were obtained by the fitting to the equation (S12):

$$I = I_{min} + \frac{I_{max} - I_{min}}{1 + \frac{c_w}{K_x \times c_l}} \qquad \text{(S12)}$$

where I_{min} is the emission intensity without vesicles, I_{max} is the maximum emission intensity that could be reached after increasing vesicles concentration, c_w is the concentration of water (55.3 M), c_l is the lipids concentration and K_x the partition coefficient.

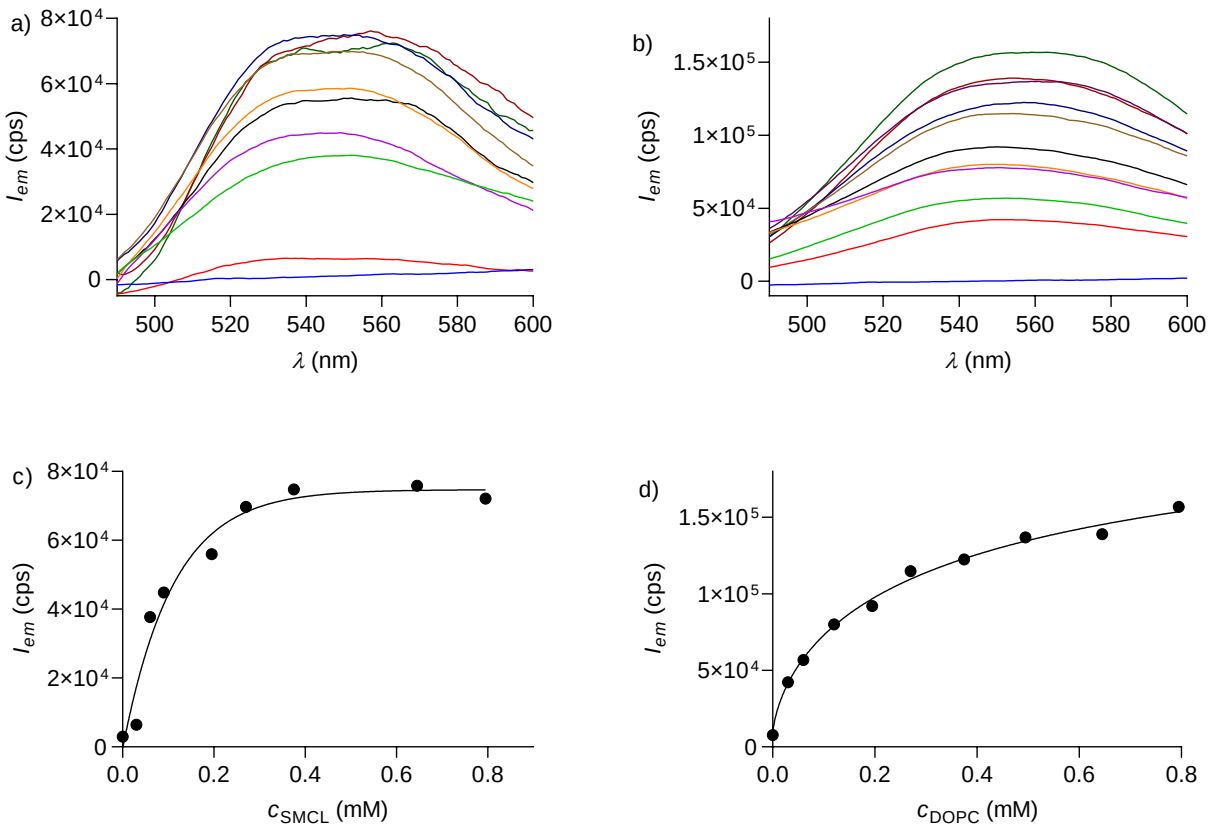

Fig. S19 Emission spectra (λ_{ex} = 425 nm) of **2** with increasing concentrations of a) SM/CL LUVs and b) DOPC LUVs. Intensity of emission at 560 nm fitted to equation (S12) in c) SM/CL LUVs (K_x = (4.1 ± 0.6) ×10^5 M^{-1}) and in d) DOPC LUVs (K_x = (5.5 ± 1.5) ×10^5 M^{-1}).

7. Cellular studies

Cell preparation. As described in reference S1, HeLa Kyoto cells were cultured in 25 cm^2 cell culture flasks and grew in DMEM + 10% FBS + 1% Pen/Strep. For microscopy experiments the cells were seeded at 8 × 10^4 cells/mL in DMEM + 10% FBS + 1% Pen/Strep on 35 mm glass bottom dishes and kept at 37 °C with 5% CO_2 overnight. Afterwards, they were washed (3 × 1 mL) and incubated

with Leibovitz's medium containing the corresponding probe at 37 °C for different time periods. If specified, additional washing with Leibovitz was performed after incubation, consisting on removing Leibovitz solution containing the probe and washing with 1 mL of fresh Leibovitz medium.

CLSM measurements. The cells were prepared as previously described and imaged with a Leica SP5 confocal microscope using an argon laser at λ_{ex} = 488 nm with the laser power at 30%. Emission was collected between 550 and 650 nm. Brightness and contrast were adjusted and it was the same for all the pictures. All images were treated with ImageJ software.

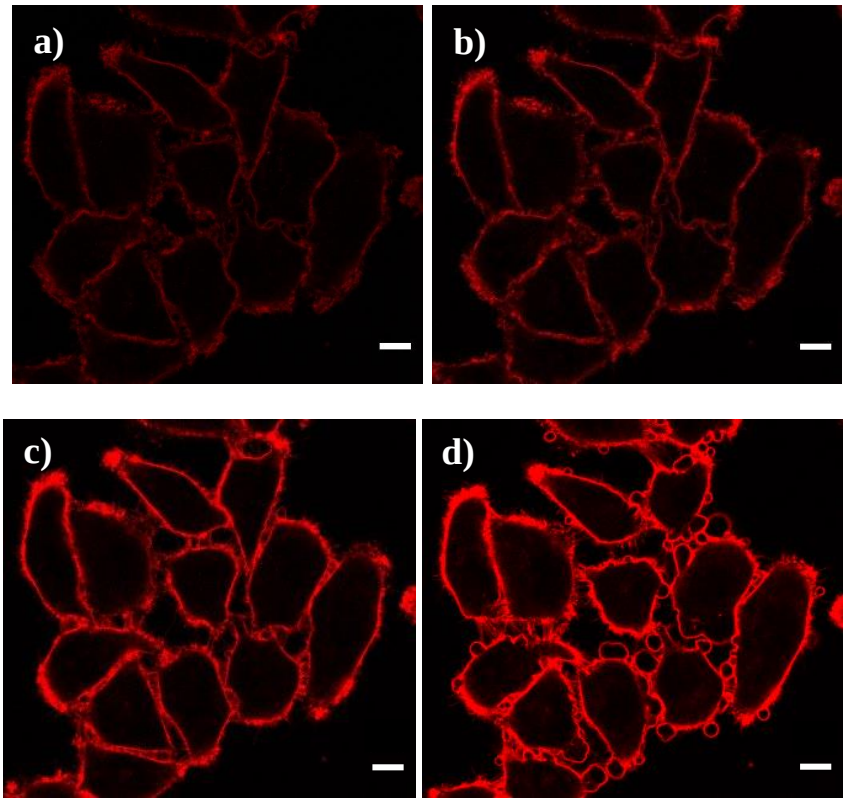

Fig. S20 CLSM images in HeLa Kyoto cells of probe **1** (4 μM) at different times after addition of the probe (a) 2 min, (b) 3 min, (c) 6 min and (d) 27 min; no washing, laser power: 30%, scale bar: 10 μm.

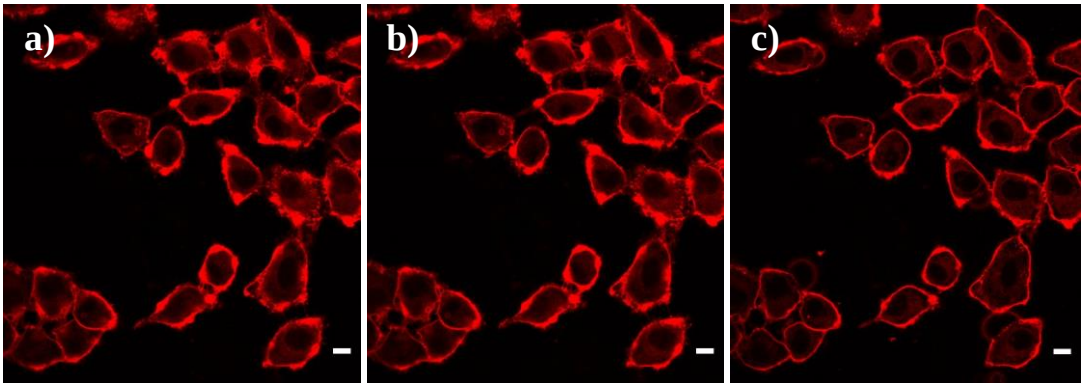

Fig. S21 CLSM images in HeLa Kyoto cells of probe **2** (4 μM) at different times after addition of the probe (a) 3 min, (b) 6 min and (c) 27 min; no washing, laser power: 30%, scale bar: 10 μm.

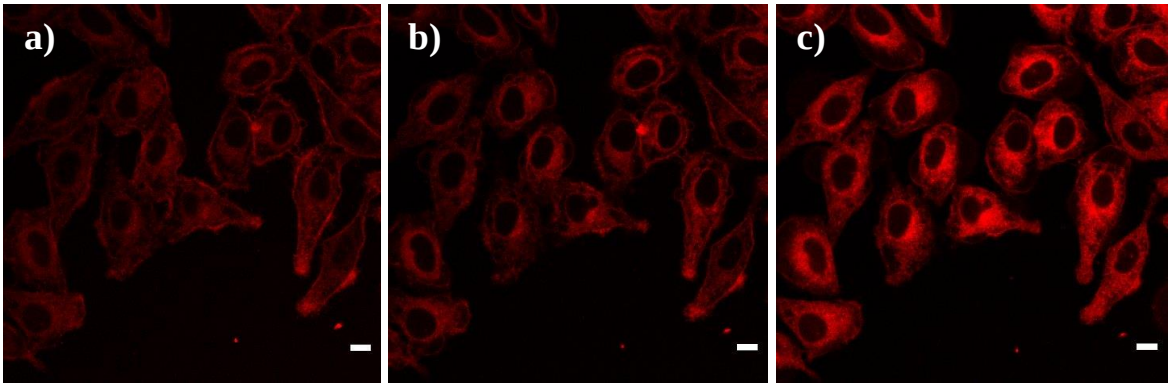

Fig. S22 CLSM images in HeLa Kyoto cells of probe **3** (4 μM) at different times after addition of the probe (a) 3 min, (b) 6 min and (c) 27 min; no washing, laser power: 30%, scale bar: 10 μm.

FLIM of HeLa Kyoto cells. Before image acquisition, HeLa Kyoto cells were incubated with probe **1** (4 μM, 3 min), probe **2** (4 μM, 30 min), or probe **3** (4 μM, 3 min) in Leibovitz's medium. FLIM images were taken before hyperosmotic shock and after 5 min of hyperosmotic treatment. The hyperosmotic shock was performed by using Leibovitz's medium containing 0.5 M of sucrose. For analysis, SymPhoTime 64 software (PicoQuant) was used to fit fluorescence decay data (from full

images, at least 10 cells per image) to a triple exponential deconvolution model, from the ROIs selected using the intensity of the fluorescence signal. Data are expressed as mean ± SD.

Table S4 Fluorescence lifetime parameters on HeLa Kyoto cellular membranes calculated before and after osmotic shock.

		τ_{av} (ns)	
Entry	Cpd[a]	Isosmotic[b]	Hyperosmotic[c]
1	**1**	4.03 ± 0.05	3.74 ± 0.03
2	**2**	1.27 ± 0.01	1.20 ± 0.01
3	**3**	0.49 ± 0.00	0.55 ± 0.01

[a]Compounds **1** – **3**. [b]Average Fluorescence lifetime in HeLa Kyoto cells under isosmotic conditions from 3 images. [c]Same after hyperosmotic conditions.

8. NMR spectra

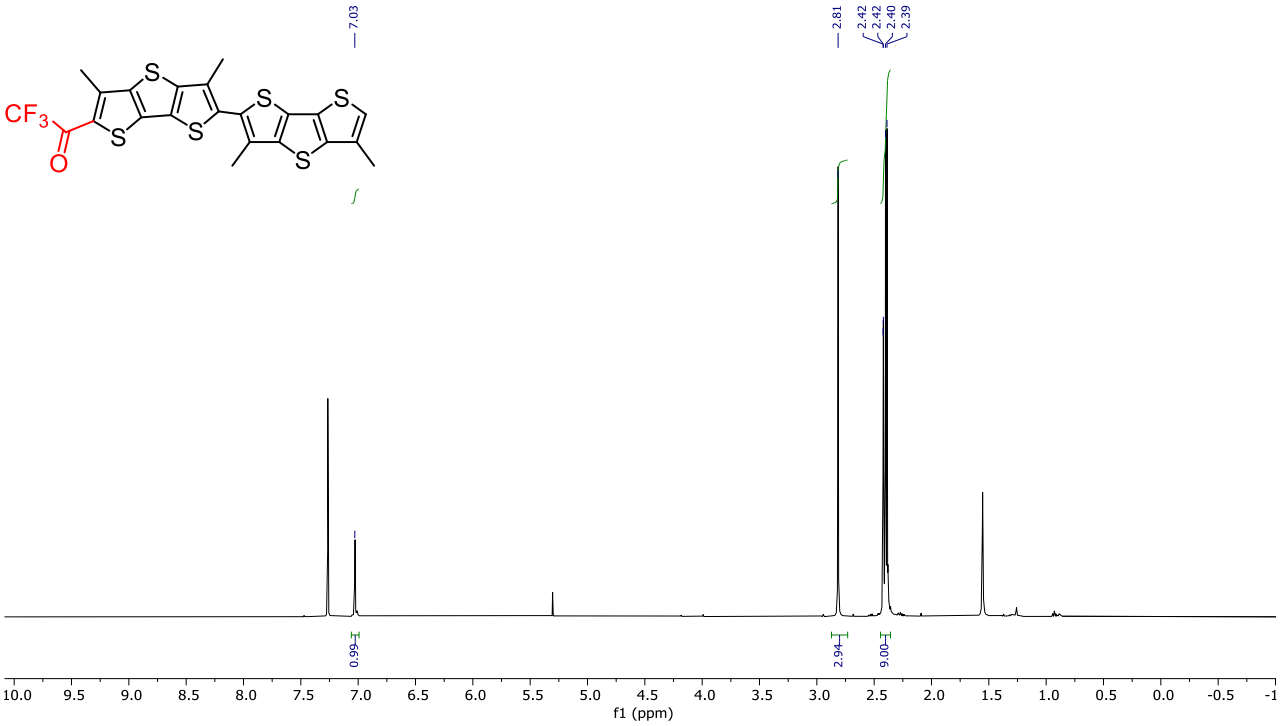

Fig. S23 ^{1}H NMR (400 MHz) spectrum of compound **8** in $CDCl_3$.

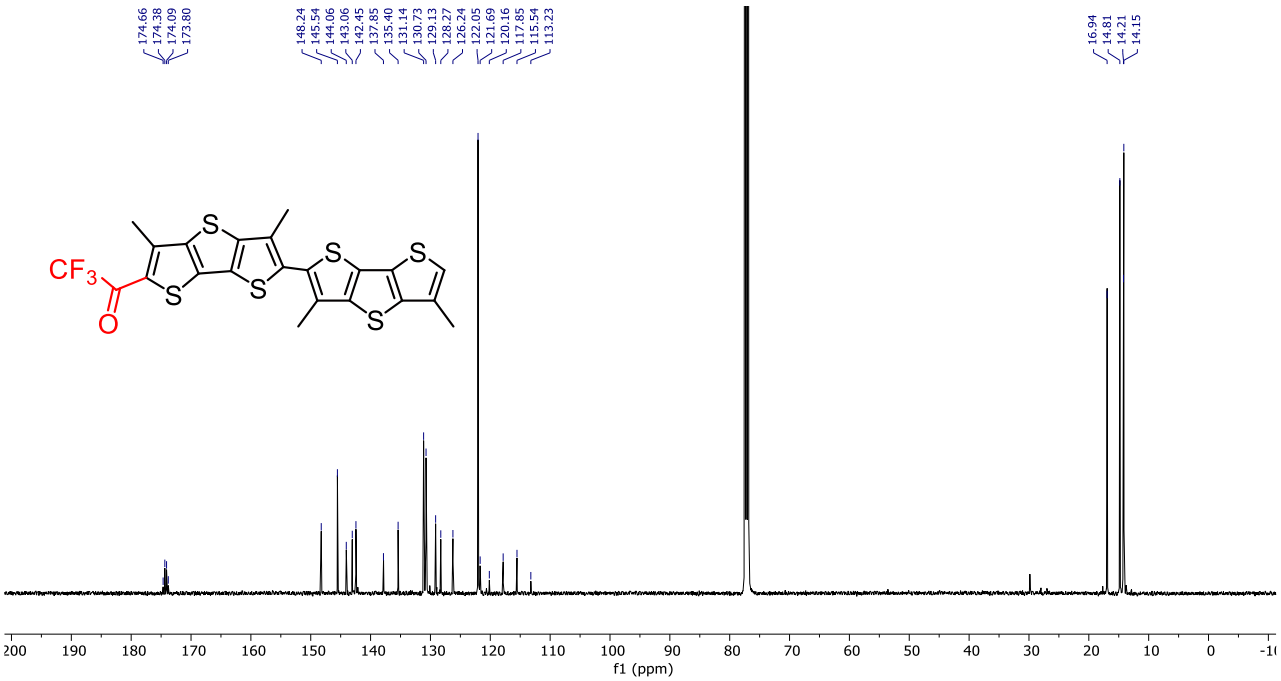

Fig. S24 ^{13}C NMR (126 MHz) spectrum of compound **8** in $CDCl_3$.

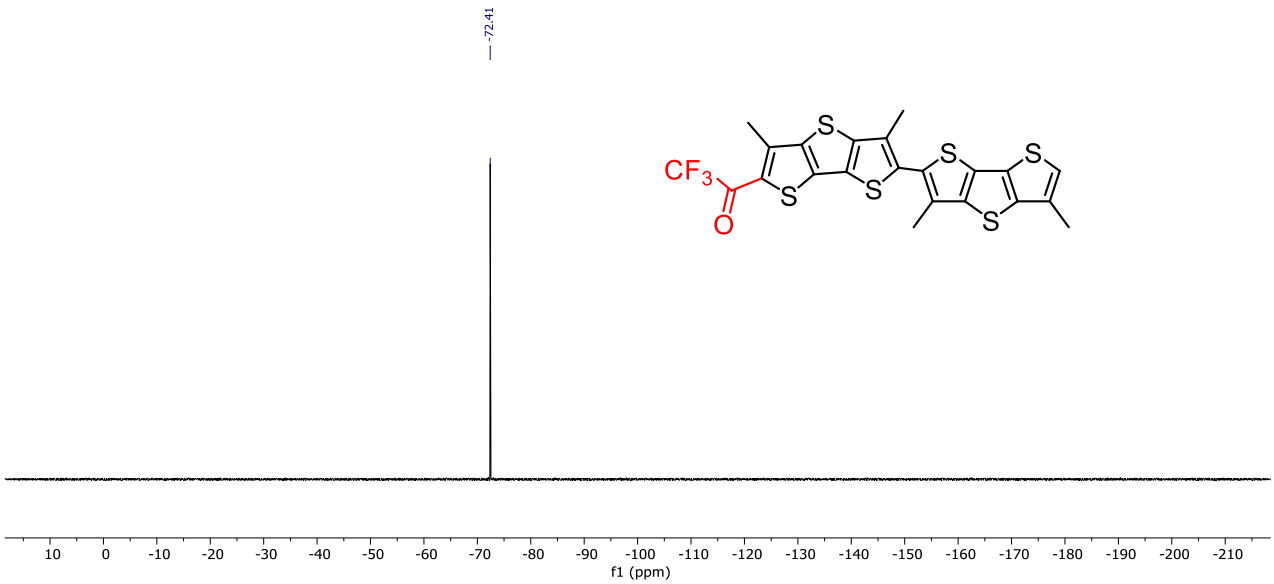

Fig. S25 ^{19}F NMR(282 MHz) spectrum of compound **8** in $CDCl_3$.

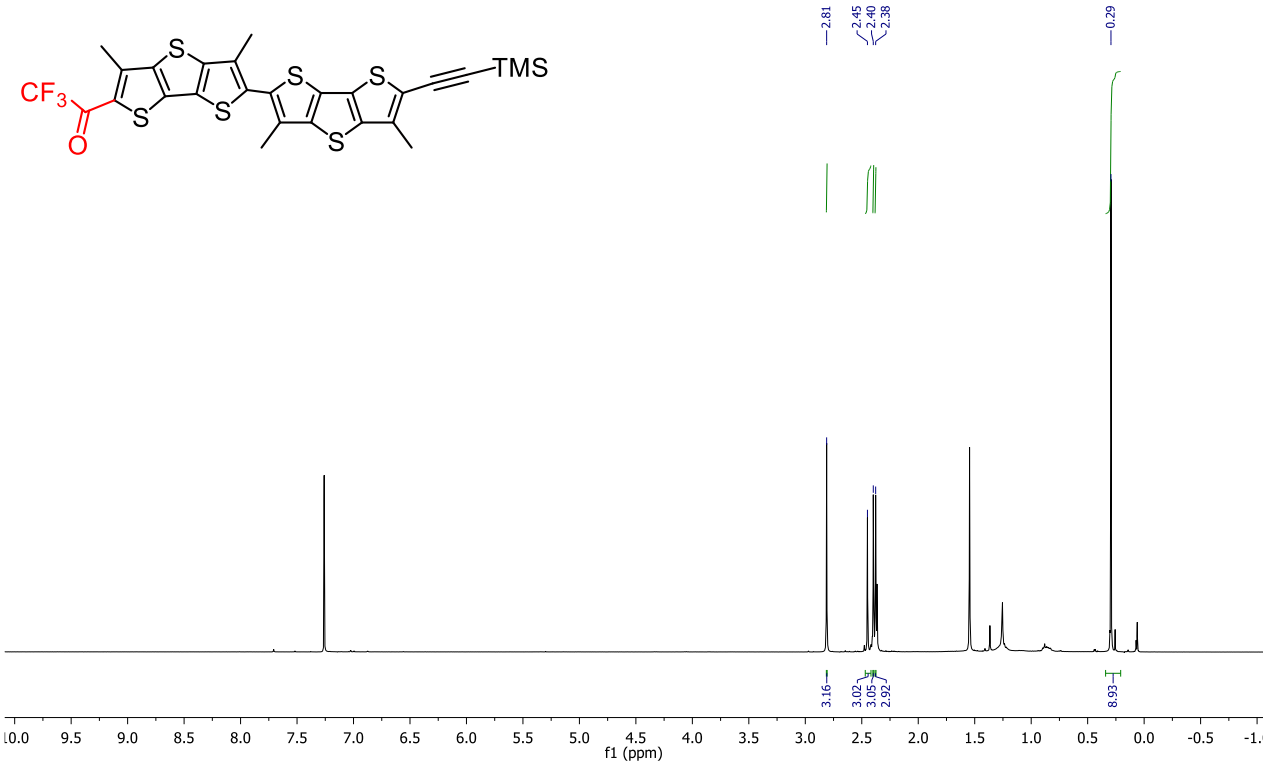

Fig. S26 ^{1}H NMR (400 MHz) spectrum of compound **16** in $CDCl_3$.

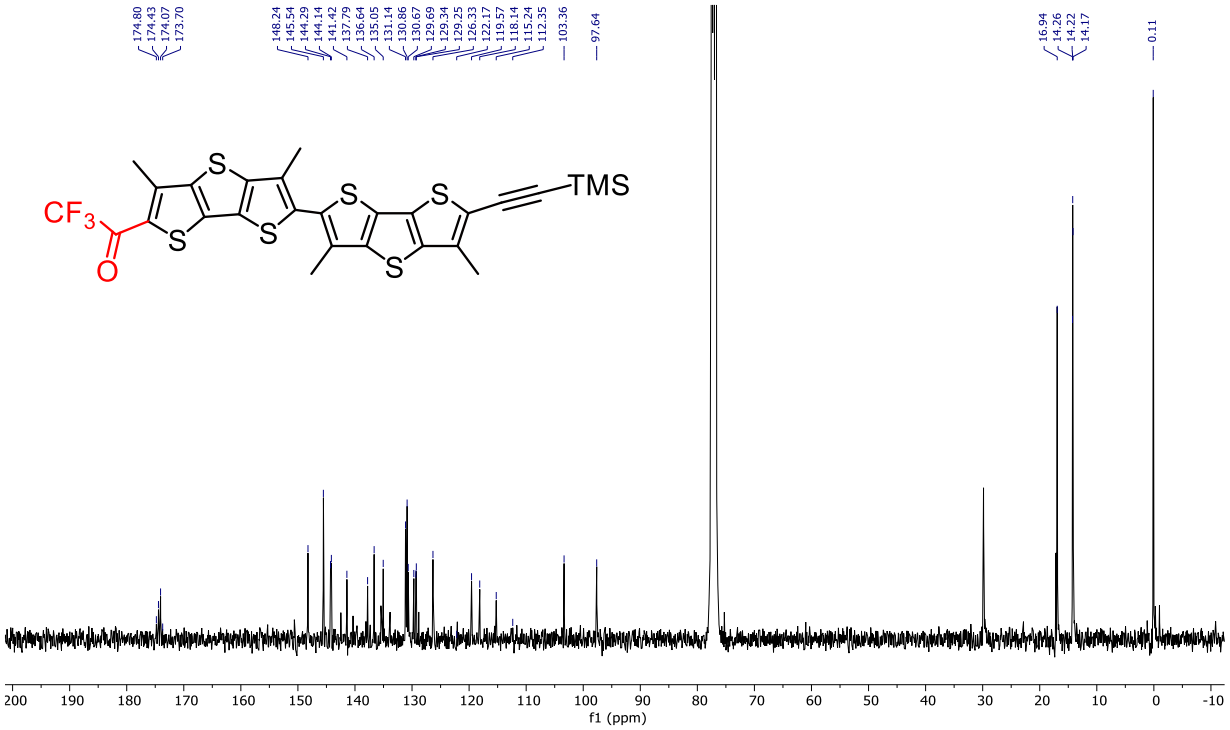

Fig. S27 ^{13}C NMR (126 MHz) spectrum of compound **16** in $CDCl_3$.

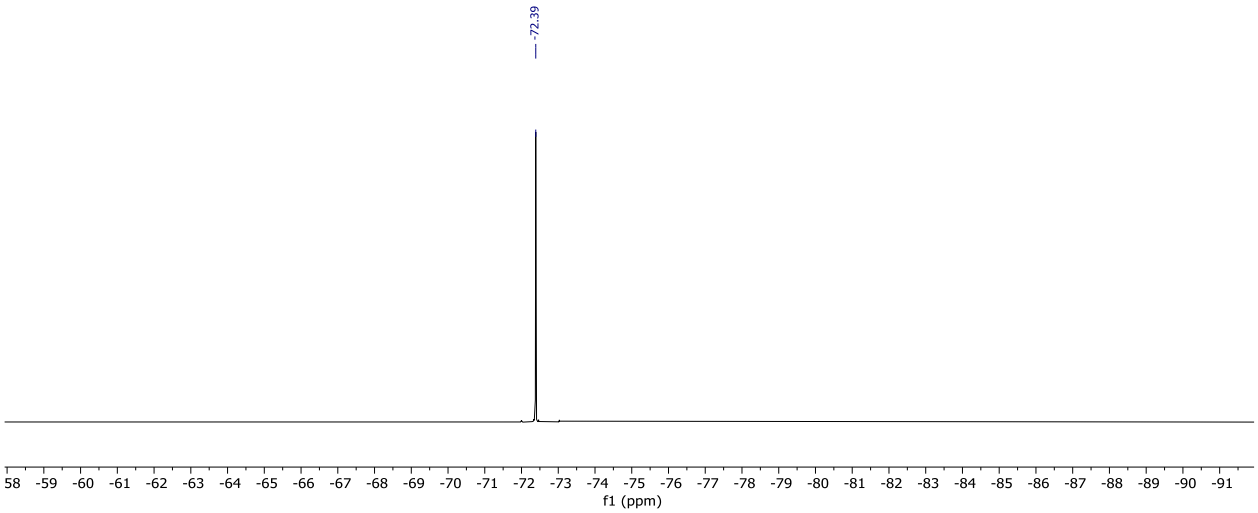

Fig. S28 ^{19}F NMR (282 MHz) spectrum of compound **16** in $CDCl_3$.

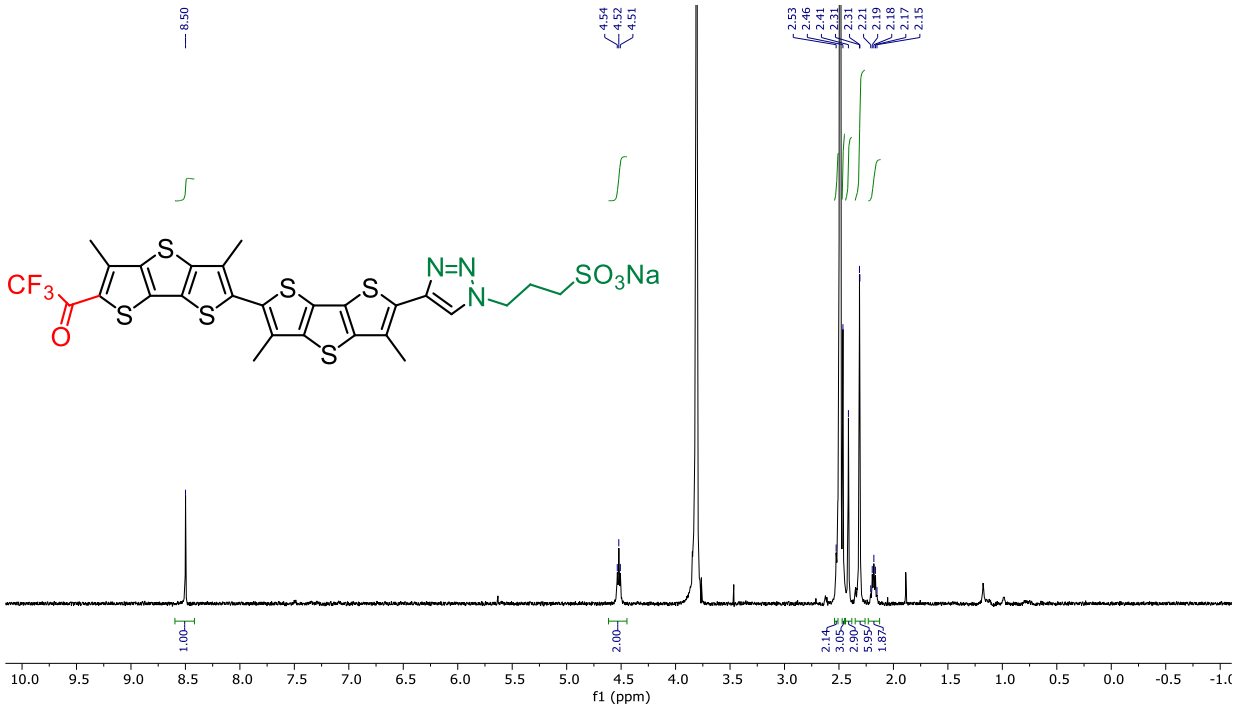

Fig. S29 ^{1}H NMR (500 MHz) spectrum of compound **2** (hydrate form) in DMSO-d_6 + 10% D_2O.

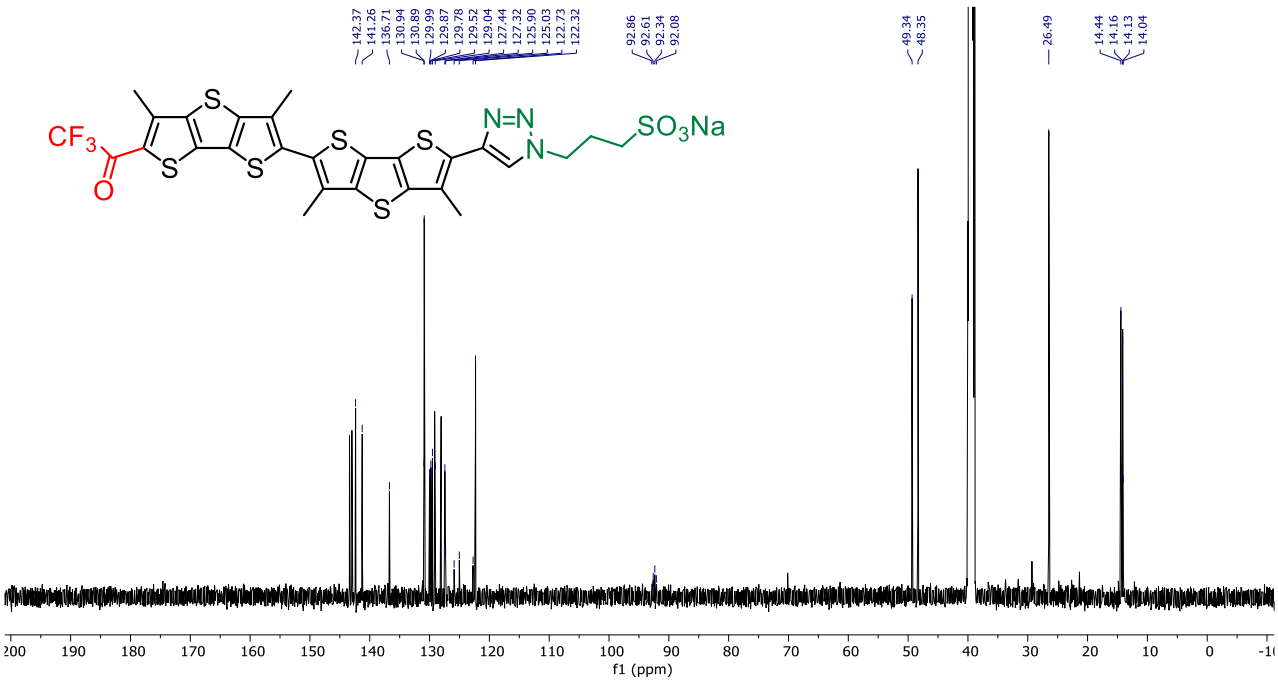

Fig. S30 ^{13}C NMR (126 MHz) spectrum of compound **2** (hydrate form) in DMSO-d_6 + 10% D_2O.

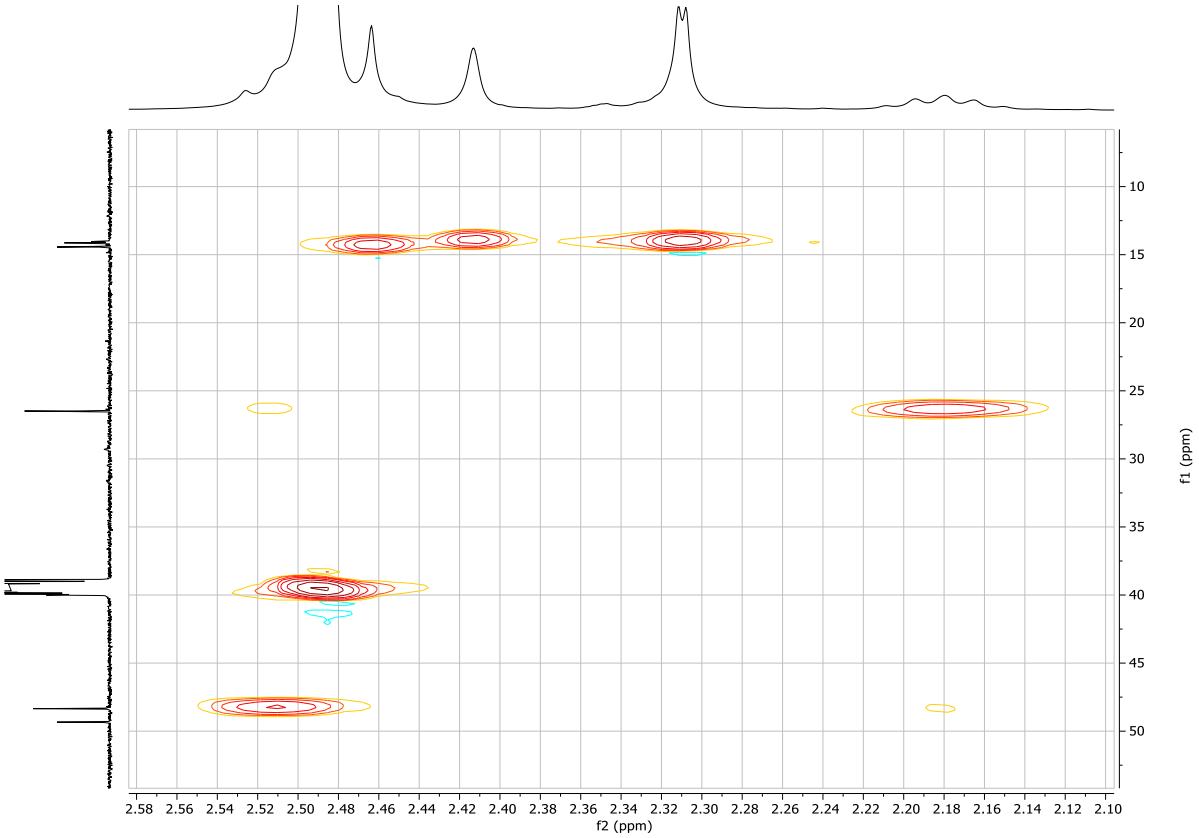

Fig. S31 HSQC spectrum of compound **2** (hydrate form) in DMSO-d_6 + 10% D_2O.

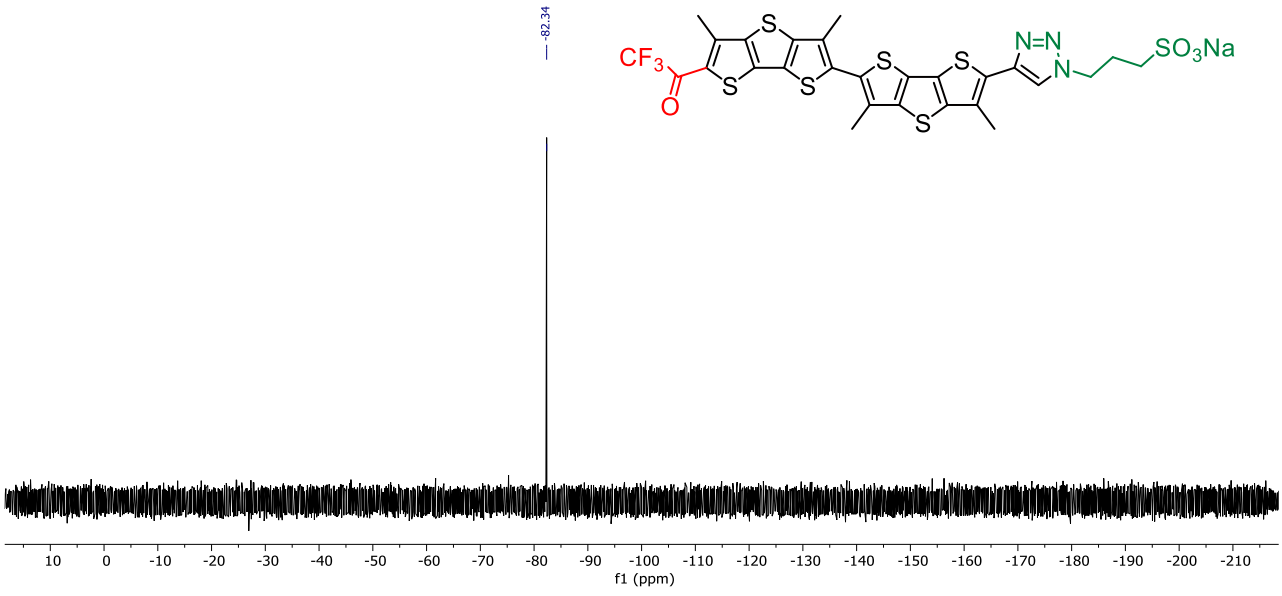

Fig. S32 ^{19}F NMR (282 MHz) spectrum of compound **2** (hydrate form) in DMSO-d_6 + 10% D_2O.

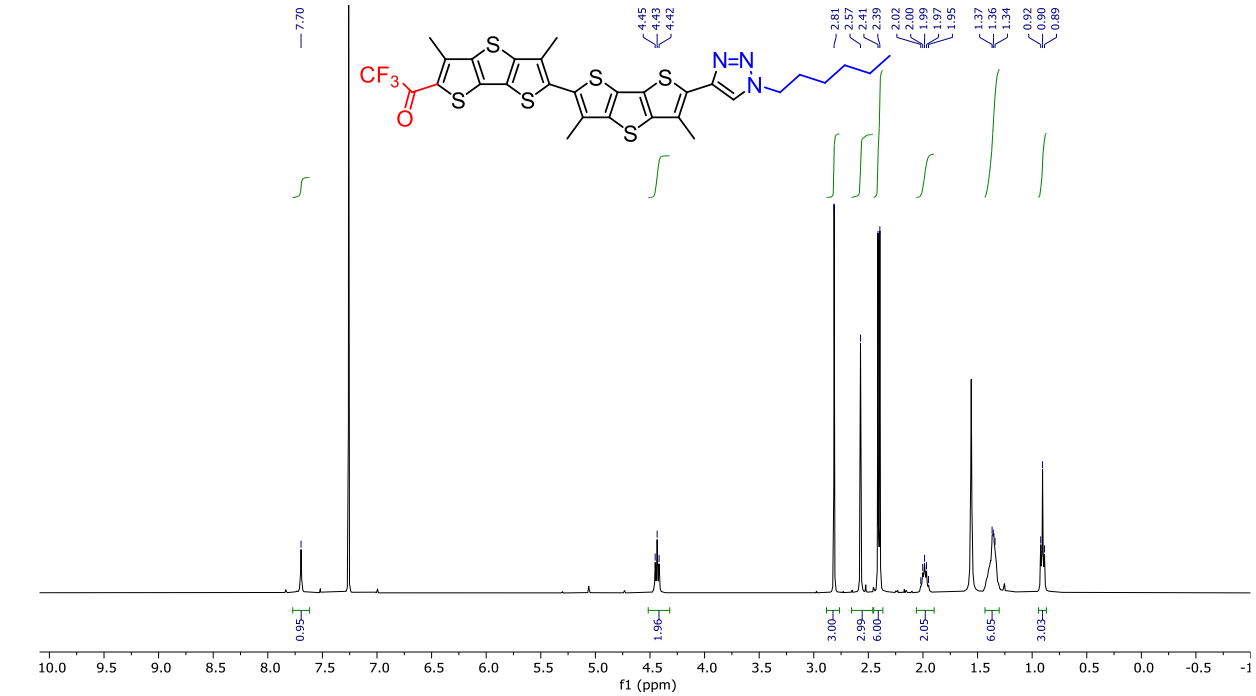

Fig. S33 ^{1}H NMR (400 MHz) spectrum of compound **2'** in $CDCl_3$.

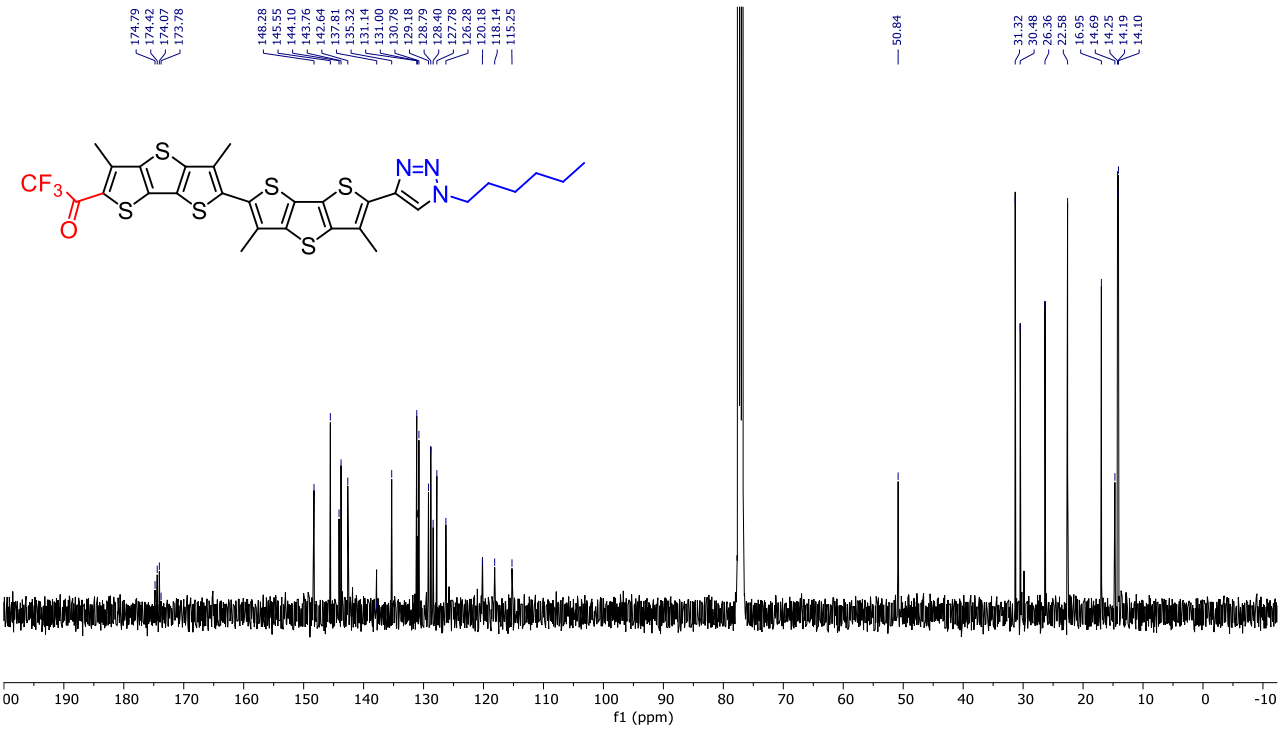

Fig. S34 ^{13}C NMR (101 MHz) spectrum of compound **2'** in $CDCl_3$.

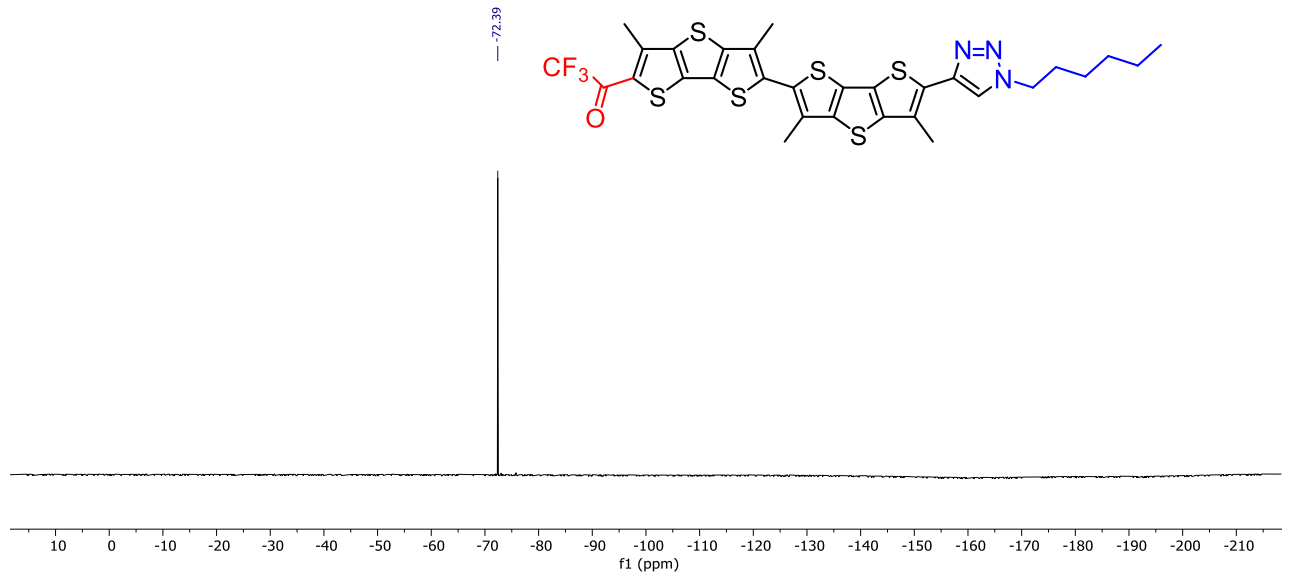

Fig. S35 ^{19}F NMR (282 MHz) spectrum of compound **5** in $CDCl_3$.

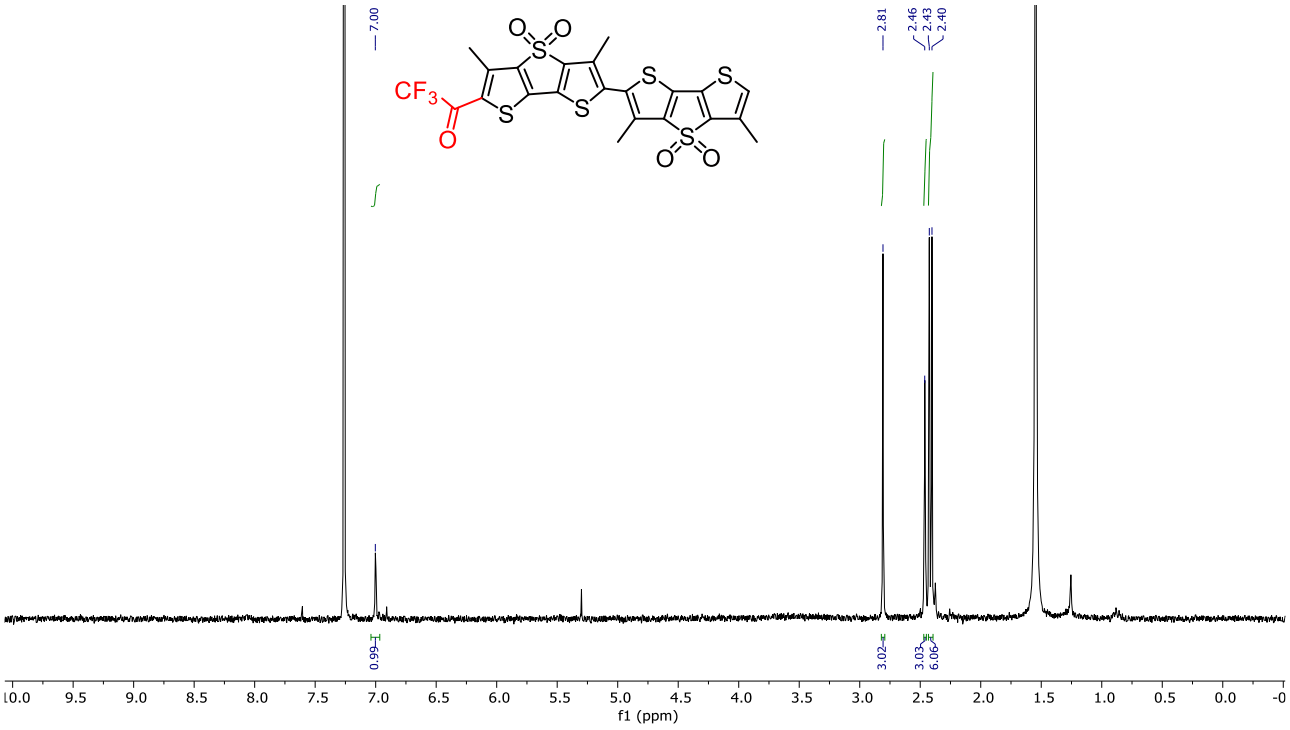

Fig. S36 ^{1}H NMR (400 MHz) spectrum of compound **10** in $CDCl_3$.

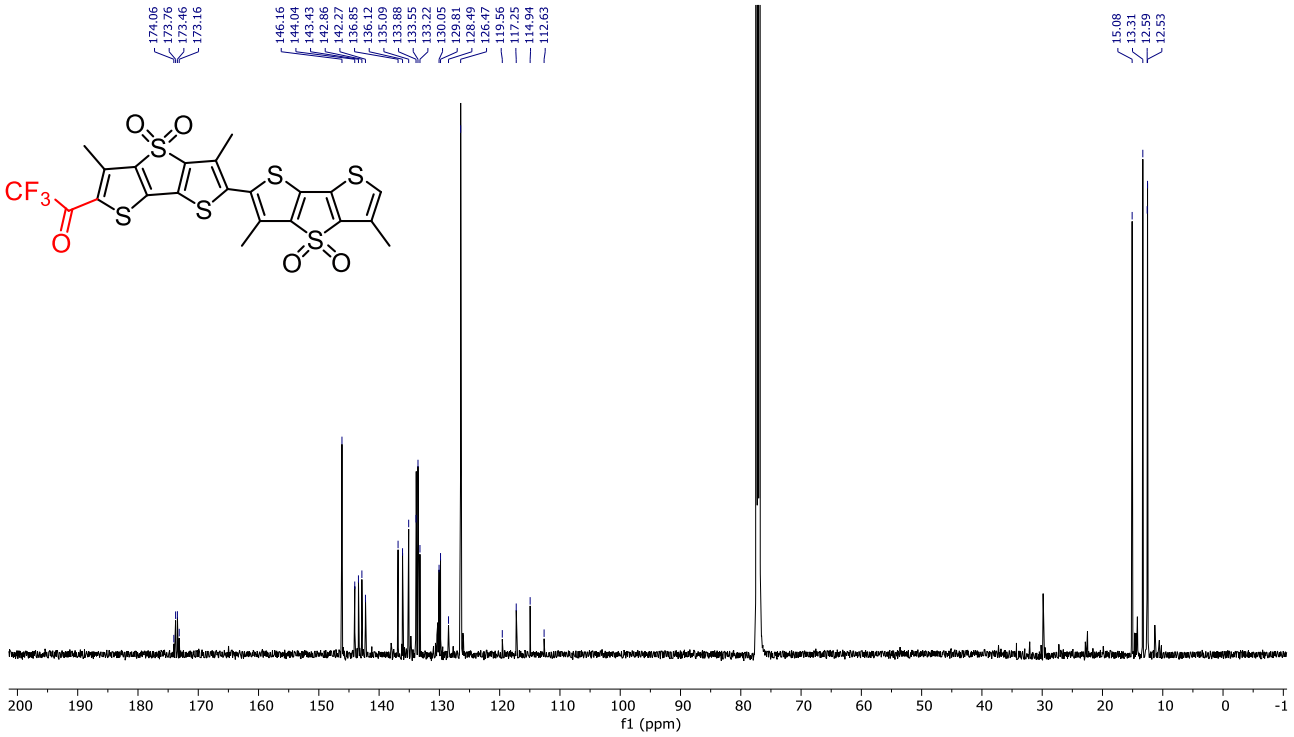

Fig. S37 ^{13}C NMR (126 MHz) spectrum of compound **10** in $CDCl_3$.

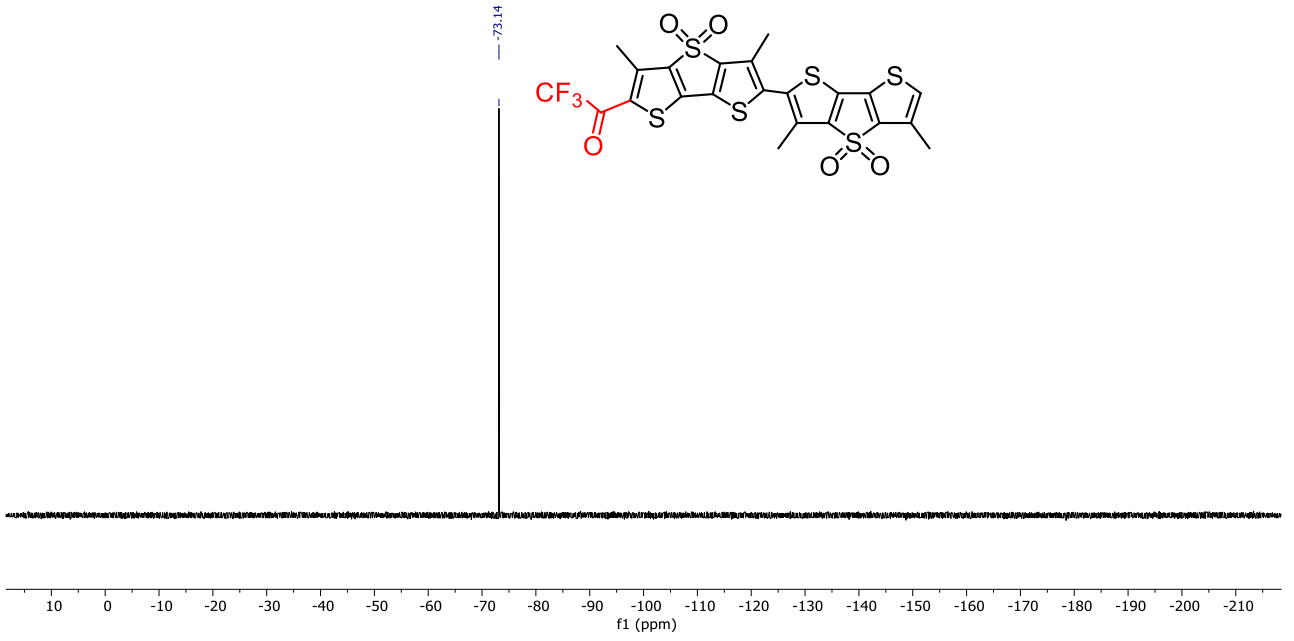

Fig. S38 ^{19}F NMR (282 MHz) spectrum of compound **10** in $CDCl_3$.

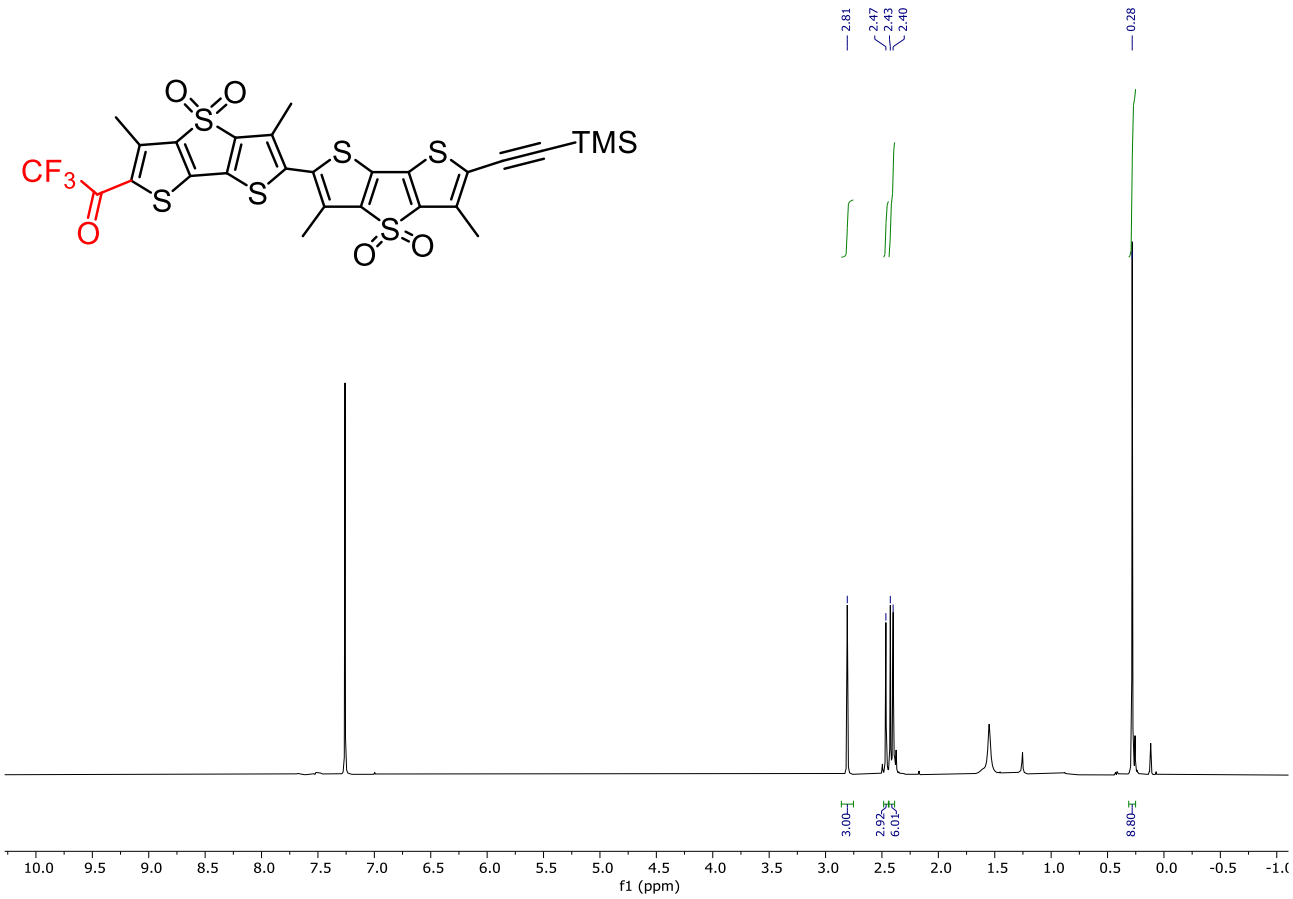

Fig. S39 ^{1}H NMR (400 MHz) spectrum of compound **18** in $CDCl_3$.

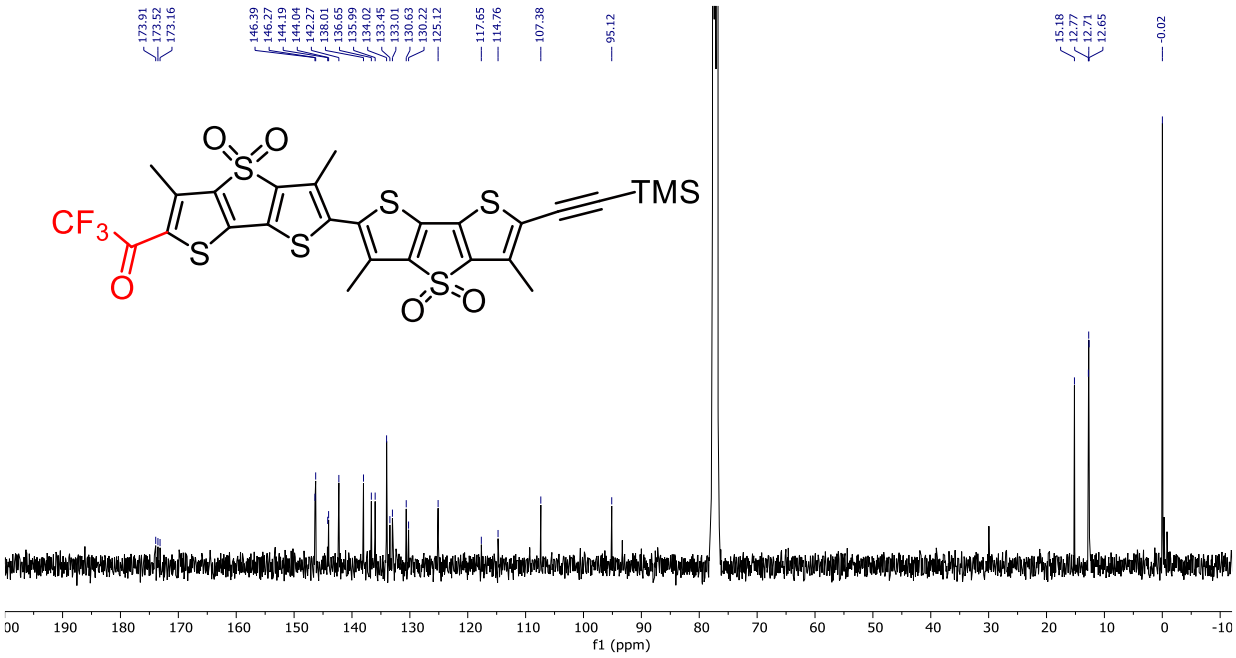

Fig. S40 ^{13}C NMR (126 MHz) spectrum of compound **18** in $CDCl_3$.

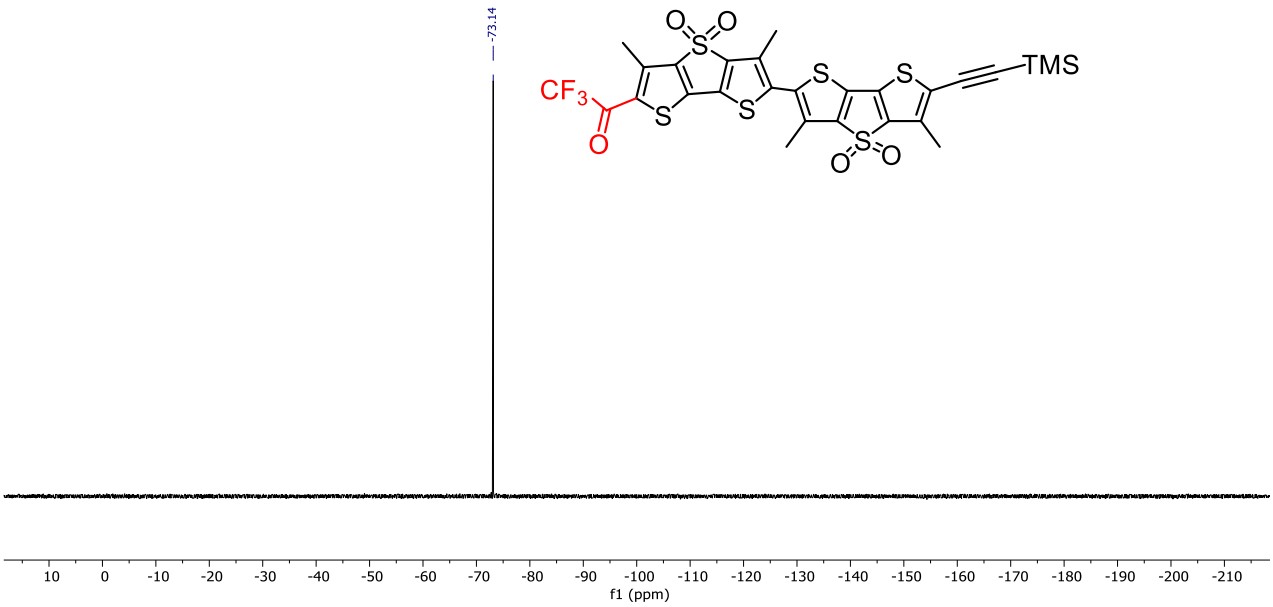

Fig. S41 ^{19}F NMR (282 MHz) spectrum of compound **18** in $CDCl_3$.

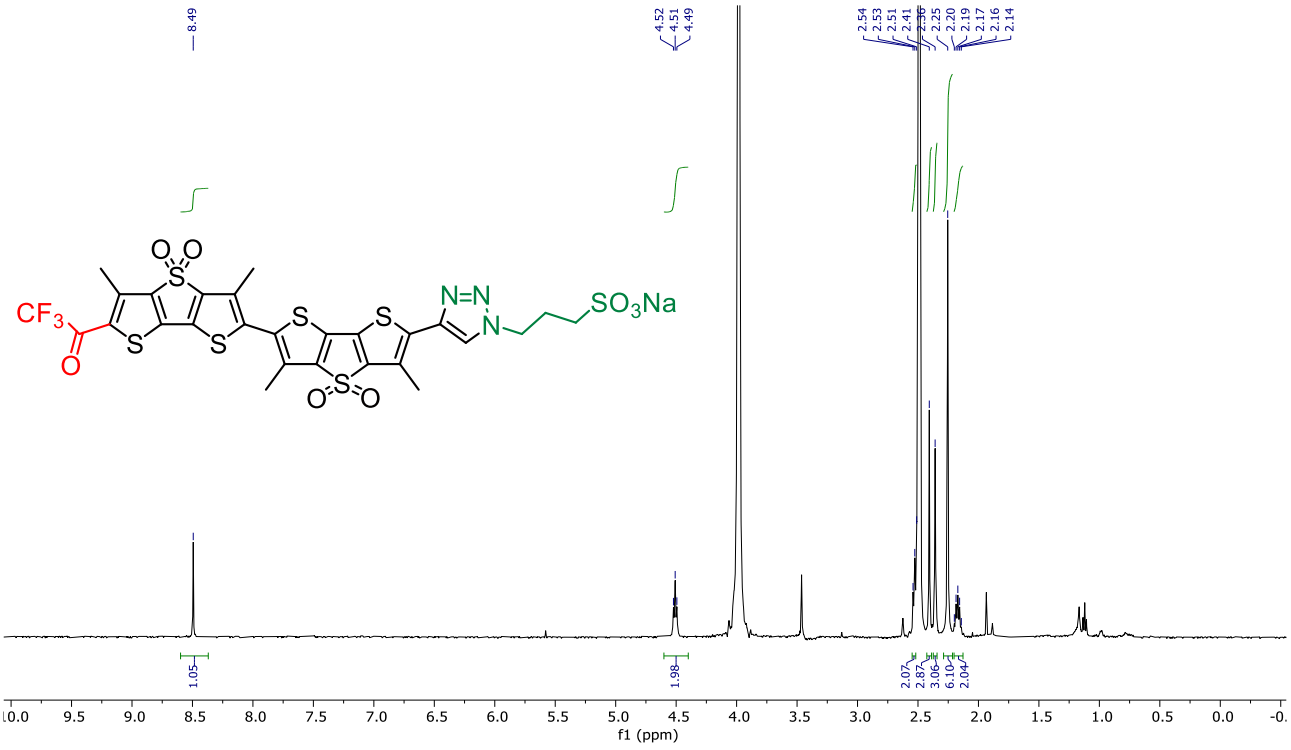

Fig. S42 ^{1}H NMR (500 MHz) spectrum of compound **3** (hydrate form) in DMSO-d_6.

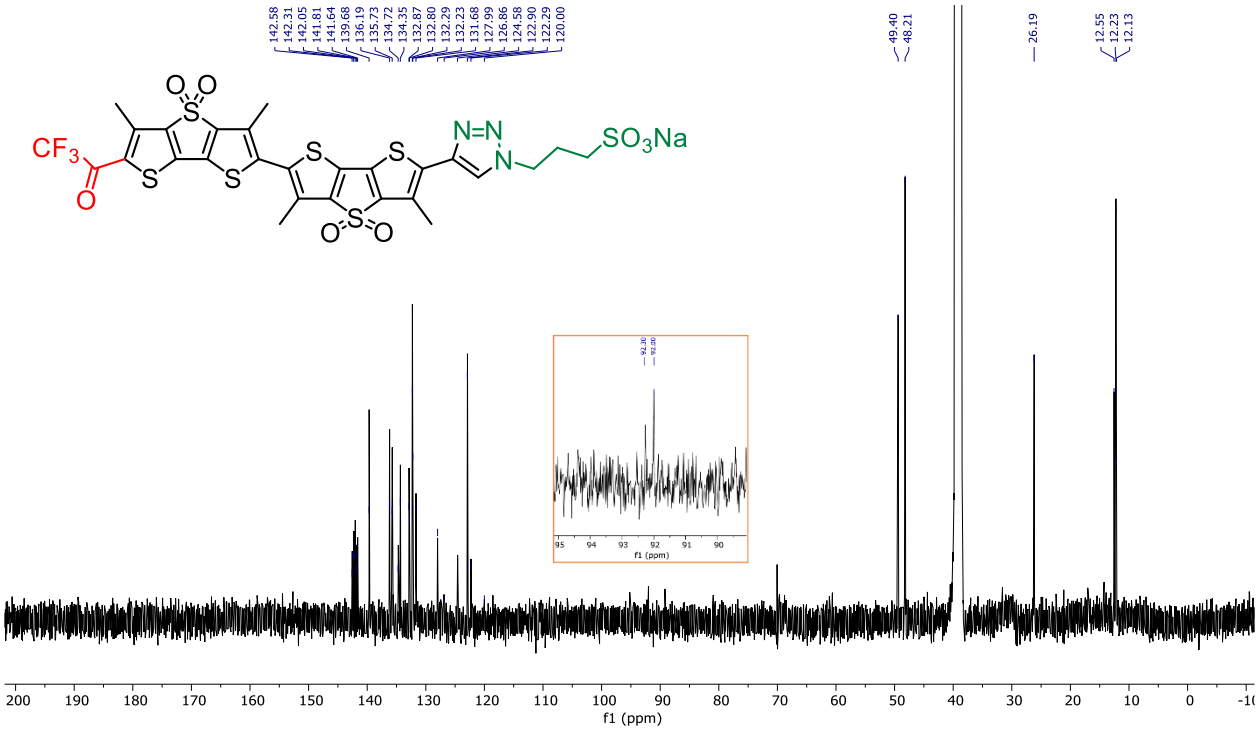

Fig. S43 ^{13}C NMR (126 MHz) spectrum of compound **3** (hydrate form) in DMSO-d_6 + 10% D_2O.

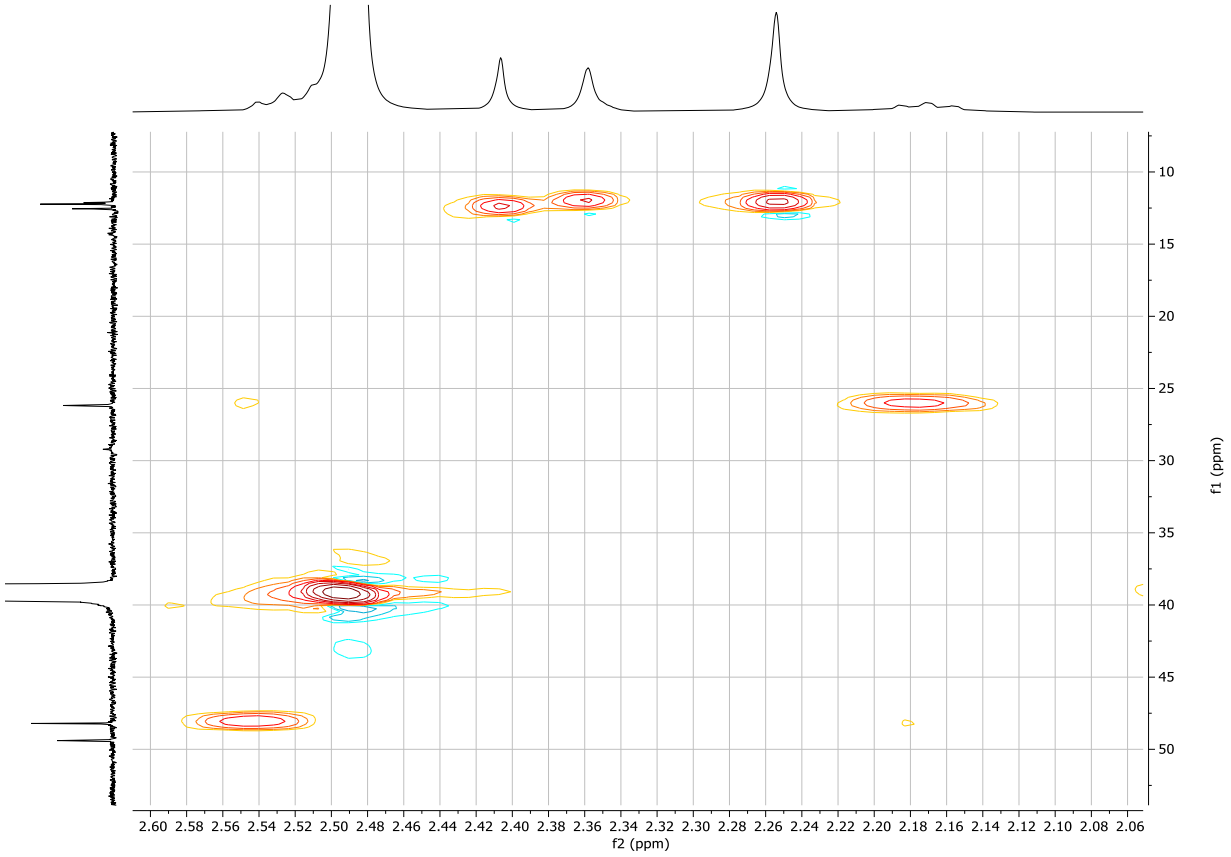

Fig. S44 HSQC spectrum of compound **3** (hydrate form) in DMSO-d_6 + 10% D_2O.

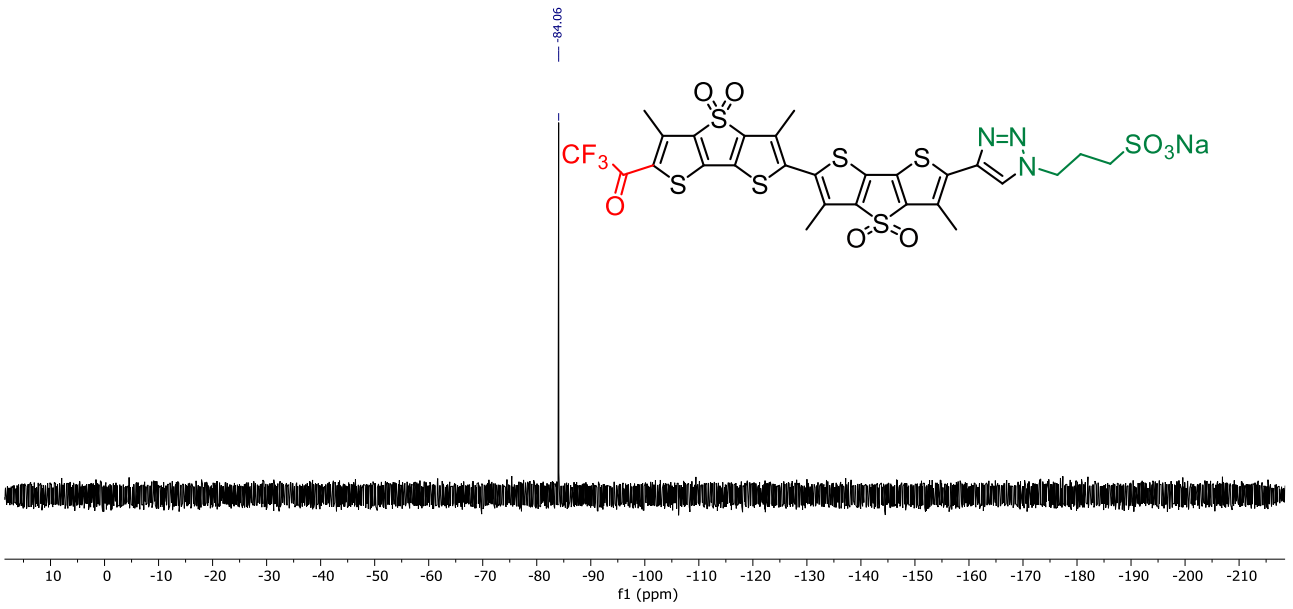

Fig. S45 ^{19}F NMR (282 MHz) spectrum of compound **3** (hydrate form) in DMSO-d_6 + 10% D_2O.

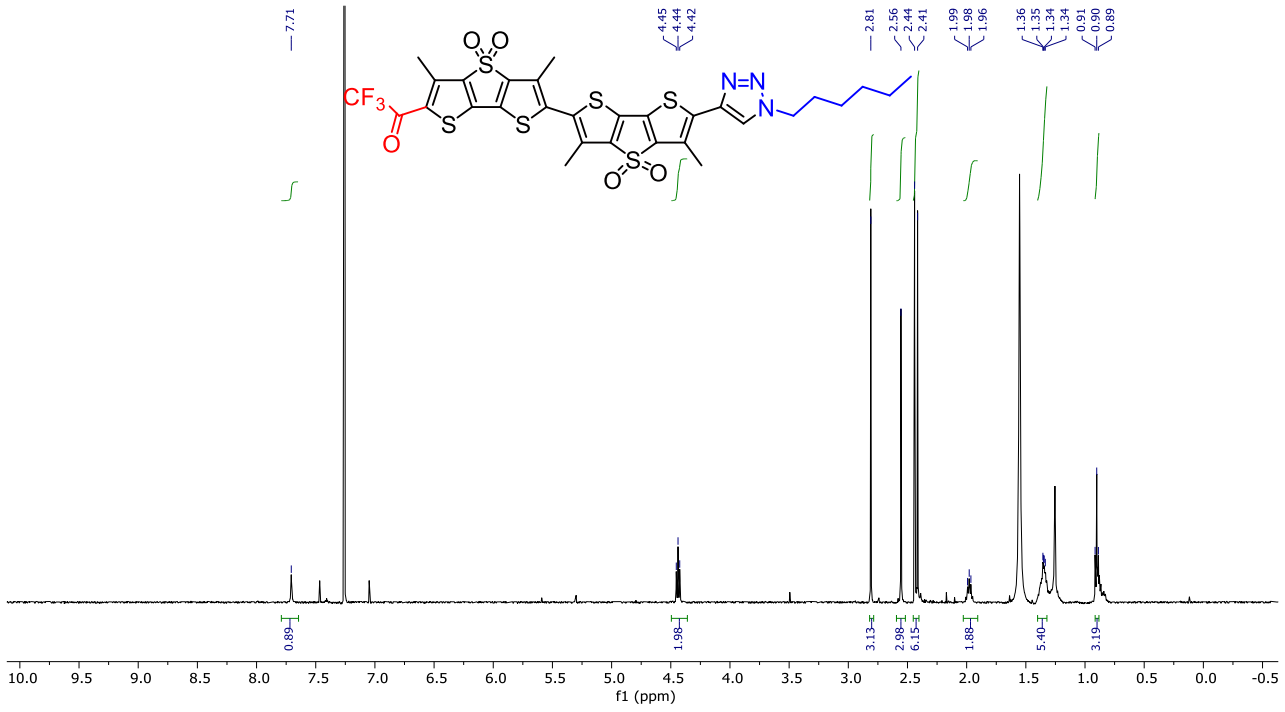

Fig. S46 ^{1}H NMR (500 MHz) spectrum of compound **3'** in $CDCl_3$.

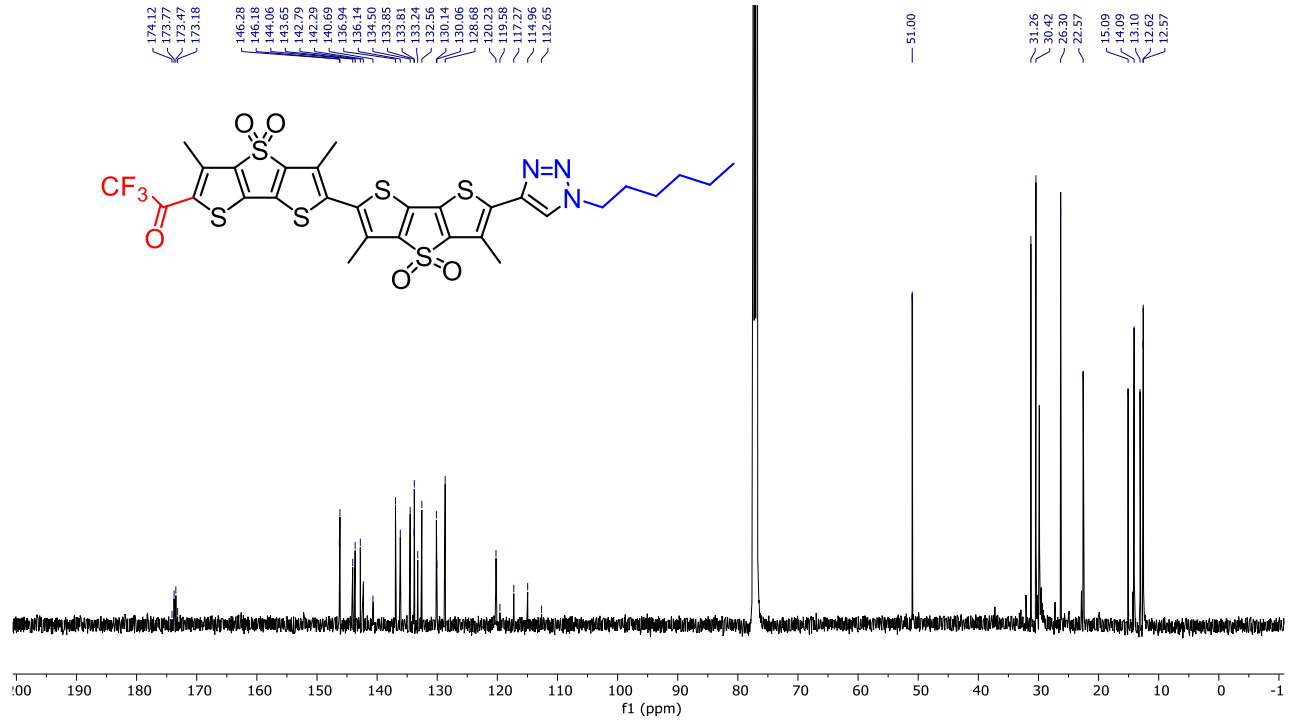

Fig. S47 ^{13}C NMR (126 MHz) spectrum of compound **3'** in $CDCl_3$.

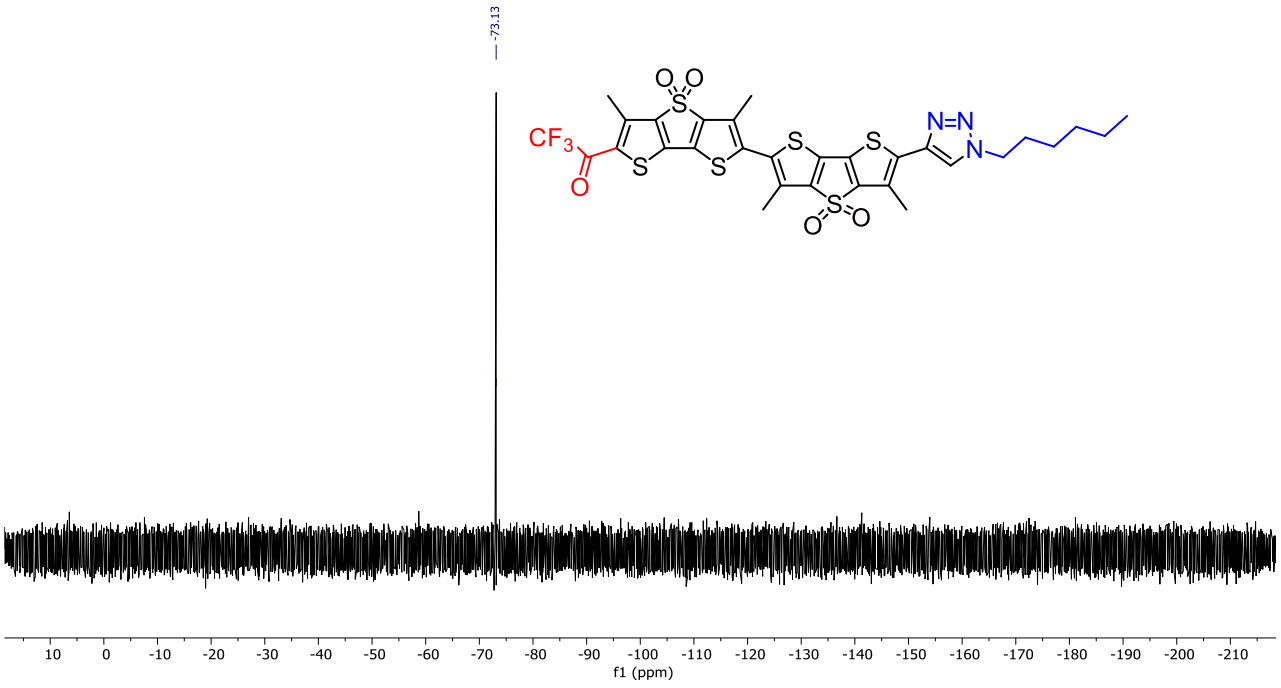

Fig. S48 ^{19}F NMR (282 MHz) spectrum of compound **3'** in $CDCl_3$.

9. Supplementary references

S1 J. García-Calvo, J. Maillard, I. Fureraj, K. Strakova, A. Colom, V. Mercier, A. Roux, E. Vauthey, N. Sakai, A. Fürstenberg and S. Matile, *J. Am. Chem. Soc.*, 2020, **142**, 12034–12038.

S2 M. Macchione, M. Tsemperouli, A. Goujon, A. R. Mallia, N. Sakai, K. Sugihara and S. Matile, *Helv. Chim. Acta*, 2018, **101**, e1800014.

S3 J. Grünewald, Y. Jin, J. Vance, J. Read, X. Wang, Y. Wan, H. Zhou, W. Ou, H. E. Klock, E. C. Peters, T. Uno, A. Brock and B. H. Geierstanger, *Chem*, 2017, **28**, 1906–1915.

S4 C. C. Vequi-Suplicy, K. Coutinho and M. T. Lamy, *Biophys. Rev.*, 2014, **6**, 63–74.

S5 K. Strakova, A. I. Poblador-Bahamonde, N. Sakai and S. Matile, *Chem. Eur. J.*, 2019, **25**, 14935–14942.

S6 M. Dal Molin, Q. Verolet, A. Colom, R. Letrun, E. Derivery, M. Gonzalez-Gaitan, E. Vauthey, A. Roux, N. Sakai and S. Matile, *J. Am. Chem. Soc.*, 2015, **137**, 568–571.

The original data can be found at:

https://dx.doi.org/10.5281/zenodo.4584732